Advanced Drug Delivery Reviews 138 (2019) 117–132

Contents lists available at ScienceDirect

Advanced Drug Delivery Reviews

journal homepage: www.elsevier.com/locate/addr

Remotely controlled opening of delivery vehicles and release of cargo by external triggers

Dingcheng Zhu [a], Sathi Roy [a], Ziyao Liu [a], Horst Weller [b], Wolfgang J. Parak [a,b], Neus Feliu [a,c,*]

[a] Fachbereich Physik, CHyN, Universität Hamburg, Hamburg, Germany
[b] Fachbereich Chemie, Universität Hamburg, Hamburg, Germany
[c] Experimental Cancer Medicine, Department of Laboratory Medicine (LABMED), Karolinska Institutet, Stockholm, Sweden

ARTICLE INFO

Article history:
Received 15 June 2018
Received in revised form 23 September 2018
Accepted 8 October 2018
Available online 11 October 2018

ABSTRACT

Tremendous efforts have been devoted to the development of future nanomedicines that can be specifically designed to incorporate responsive elements that undergo modification in structural properties upon external triggers. One potential use of such stimuli-responsive materials is to release encapsulated cargo upon excitation by an external trigger. Today, such stimuli-response materials allow for spatial and temporal tunability, which enables the controlled delivery of compounds in a specific and dose-dependent manner. This potentially is of great interest for medicine (*e.g.* allowing for remotely controlled drug delivery to cells, *etc.*). Among the different external exogenous and endogenous stimuli used to control the desired release, light and magnetic fields offer interesting possibilities, allowing defined, real time control of intracellular releases. In this review we highlight the use of stimuli-responsive controlled release systems that are able to respond to light and magnetic field triggers for controlling the release of encapsulated cargo inside cells. We discuss established approaches and technologies and describe prominent examples. Special attention is devoted towards polymer capsules and polymer vesicles as containers for encapsulated cargo molecules. The advantages and disadvantages of this methodology in both, *in vitro* and *in vivo* models are discussed. An overview of challenges associate with the successful translation of those stimuli-responsive materials towards future applications in the direction of potential clinical use is given.

Contents

1. Introduction

Controlled delivery of small and macromolecular drugs into cells, still remains a major challenge concerning future applications of nanoparticle-based delivery systems. There are several approaches described for delivery of cargo to intracellular regions, including viral and nonviral chemical methods [1]. However, as most nanoparticle-based delivery vehicles will enter intracellular endosomes/lysosomes, cargo release into the cytosol imposes an important experimental hurdle [2]. Thus, release of encapsulated cargo from a container upon external triggers typically would release the cargo inside endosomes/

* Corresponding author.
E-mail address: nfeliu@physnet.uni-hamburg.de (N. Feliu).

https://doi.org/10.1016/j.addr.2018.10.003
0169-409X/

lysosomes, and subsequent endosomal escape is needed. In fact, a desired delivery strategy would involve both opening of containers and endosomal release upon the same applied external trigger.

Starting from a general point of view, control of the site and kinetics of release is important. Today, several biomedical applications, especially those related to treatment and sensing, rely on the effective lateral and temporal control of releasing the active cargo/element, *e.g.* drugs for treatment and reporter molecules for sensing. Targeted delivery combined with controlled release thus has gained increased attention. From this perspective, therapeutic delivery systems should aim to deliver agents to the site of interest in an efficient, safe, and control manner. In general, controlled release systems are designed i) to prevent the degradation and elimination of the cargo before it has reached the target site, ii) to enhance delivery to the desired region by minimizing the exposure to non-targeted sites, and iii) to provide greater control of the local concentration of delivered cargo over the time [3]. One appealing approach to control the release of cargo from the delivery vehicle is to design an external trigger. Upon stimulation, triggering would regulate the delivery in terms of time, release, and dose at the site of action.

There are several stimuli-responsive vehicles allowing for triggering release. A variety of stimuli have been investigated to promote the release of encapsulated cargo including i) chemical cues such as local redox-conditions, pH, salt-concentrations, presence of certain DNA sequences, *etc.* [4–6] and ii) those using stimuli by physical triggers such as ultrasound, light, electric fields, magnetic fields, microwaves, heat, *etc.* [6–10]. In particular, the opportunities for controlled release using light and alternating magnetic fields as stimuli have attracted considerable attention, to which focus in this review will be given. For the use of the other triggers we refer to the literature [11–15]. For instance, light can induce local heating of plasmonic nanoparticles (NPs) entrapped in hybrid matrix, which may trigger thermal degradation of the matrix leading to controlled release of encapsulated cargo [6,16]. In a similar manner, heating can also be achieved by magnetic NPs exposed to alternating magnetic fields, also resulting in controlled release of encapsulated cargo [17]. It needs to be mentioned that the intrinsic magnetoelectricity of some magnetic NPs also enables remotely controlled delivery without employing heat [18].

As stated, the use of light as external stimulus is an interesting avenue due to its clinical applicability. Light can be manipulated with high control and precision, and itself has therapeutic applications. The successful use of light as trigger relies on the light source, in terms of wavelength, power, pulse length, *etc.* and on the physicochemical properties of the carrier NPs and the encapsulated cargo [19]. All together will determine tissue penetration, efficacy, and potential toxicity of the system. In general, light with short wavelengths has high energy. Ultraviolet (UV) light for example may cleave chemical bonds [20–22]. However, due to poor tissue penetration [23] and photo-damage to cells [24], applicability of UV light as a trigger for *in vivo* release is quite limited. In contrast, light with higher wavelength, such as in the near infrared (NIR), presents higher tissue penetration and less photodamage to cells [23], but in general shows lower ability to disrupt chemical structures [19,25].

On the other hand, carrier vehicles comprising magnetic NPs are also prominent examples of stimulus-controlled containers, which can be remotely controlled by magnetic fields. Magnetic fields can penetrate tissue and thus stimulation deep inside tissue is possible. Controlled release can be achieved using frequencies and magnetic field settings biocompatible with the human body. For instance, magneto-electric NPs, which could be controlled by both magnetic and electric fields, have been demonstrated as on-demand release materials with a site-specific delivery of drugs, such as peptides [26], and other compounds [18,27,28] into the target site.

In this review we highlight the use of light and magnetic fields to control release of encapsulated content involving both *in vitro* and *in vivo* systems. We first provide an overview of different triggers using light stimuli. For that, prominent examples of photo-responsive hybrid materials which have been applied in that context will be described. Second, we present a summary of release upon magnetic stimuli. Finally, an overview of major advantages and disadvantages of light and magnetic fields as triggers for controlled release will be given. Future perspectives and challenges needed for the development of those approaches towards their successful clinical translation will be discussed.

2. Carrier vehicle disintegration and endo/lysosomal escape of released molecular cargo

Particulate delivery vehicles, including NPs, polyelectrolyte capsules, liposomes, polyplexes, lipoplexes, *etc.* are internalized by cells *via* different endocytic pathways [29], whereby most vehicles eventually reach lysosomes [30–32]. Extensive work has been focused on developing biodegradable vehicles [29], with the goal of achieving lysosomal escape without external stimuli [7,33–35]. As an example, self-quenched DQ-ovalbumin (DQ-OVA, ~ 45 kDa, Thermofisher) [36], which according to the manufacturer is a fluorogenic substrate for proteases, was encapsulated into non-degradable poly(styrenesulfonate)/poly(allylamine hydrochloride) (PSS/PAH) or bio-degradable dextran sulfate/poly-L-arginine (DEXS/PARG) microcapsules [37]. DQ-OVA comprises ovalbumin heavily labelled with BODIPY dyes. The green fluorescence of DQ-OVA is significantly self-quenched due to saturated conjugation and thus close proximity of BODIPY molecules, in addition to red fluorescence. Upon enzymatic degradation of DQ-OVA into peptide fragments the green fluorescence is restored. Internalized capsules are endocytosed and thus exposed to proteases inside lysosome. The PSS/PAH capsules were resistant against enzymatic degradation and thus prevented DQ-OVA from degradation (Fig. 1a). In contrast, both, DEXS/PARG capsules and encapsulated DQ-OVA were almost completely degraded after 3–5 days (Fig. 1b). However, most of DQ-OVA fragments were still trapped inside lysosomes, ultimately leading to exocytosis. Similar results have also been observed by encapsulating green fluorescent protein (GFP) [38], indicating that degradation of the carrier vehicle does not necessarily involve efficient release of encapsulated cargo into the cytosol. This has been in particular investigated in the context of gene delivery. Quantitative analysis utilizing time-lapse fluorescence microscopy and electron microscopy data by Gilleron *et al.* indicated that less than 2% of siRNA delivered by lipid NPs were able to escape from in a given narrow window of time [32]. Similarly, live cell imaging showed that only few polyethylenimine (PEI)/siRNA polyplexes may efficiently release siRNA into the cytosol and subsequently lead to accumulation inside the nucleus [39]. These studies indicate that carrier opening and especially subsequent cargo escape from lysosomes are efficiency-limiting steps for molecular release to the cytosol. Similarity, Quarta *et al.* indicated that the lysosomes can degrade multilayered magnetic nanobeads loaded with DQ-OVA, leading to the proteolytic digestion of DQ-OVA. However, in this study, the authors showed that the digested products of DQ-OVA in the endosomal compartments were further released intracellularly [36]. Those studies reflected the paradigm of lysosomal escape and the need of further studies to address this relevance question.

3. Light-triggered release

In this section, several light-responsive materials and different approaches towards triggered release are discussed. However, as endosomal escape is a general problem [2], we start by describing first this common limitation of drug delivery systems, before discussing how light-triggered release may circumnavigate it.

3.1. Concepts for light-induced release

Conventional delivery vehicles as discussed have several drawbacks, including lack of temporal control of the release of encapsulated

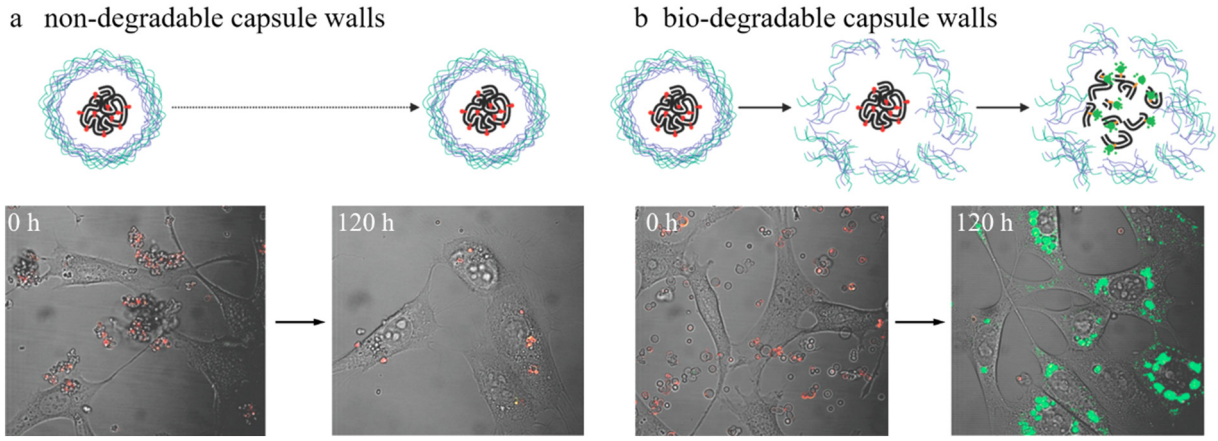

Fig. 1. Enzymatic cleavage of protein cargo. Embryonic NIH/3 T3 fibroblasts were incubated with (a) nondegradable PSS/PAH or (b) degradable DEXS/PARG capsules encapsulating DQ-OVA. Images were taken 0 h and 120 h after capsules exposure. Adapted with permission from Rivera Gil *et al.* [37].

molecules, low endo/lysosomal escape efficiency, *etc.*, which limits their versatility. Hence, inclusion of motives for external stimulation into the delivery vehicles is desirable. Among different stimuli, light is of outstanding significance as it allows for spatiotemporal control, and it can be applied in a tunable manner by selecting wavelengths, polarization direction, intensities, light spot size, pulsed laser *versus* continuous irradiation, *etc.* In case the light intensity and duration of the trigger is much lower than that for photodynamic therapy (PDT) and photothermal therapy (PTT), these strategies would avoid causing direct cell death [40], deactivation of nucleic acids [40,41] or proteins [38].

Extensive efforts have been devoted to engineer photo-responsive systems to achieve on-demand release. Generally, at least four strategies have been developed to achieve light-mediated delivery and opening of carrier vehicles. (i) Photocleavable polymers under UV-light irradiation have been demonstrated, containing photoliable groups including o-nitrobenzaldehyde [20,21], thioacetal ortho-nitrobenzaldehyde [42], amino coumarin derivatives [43,44], or benzoin-derived diol linkers [45]. For instance, human insulin was linked to hydrophobic polymer microbeads through nitrobenzyl ester linkage. After intradermal injection, the insulin was released into the bloodstream to maintain the blood glucose level upon 2 min transcutaneous irradiation at 365 nm [46]. (ii) Photo-switchable size changes were harnessed. As example, hydrophobic spiopyran can reversibly switch to hydrophilic zwitterionic merocyanine when exposed by UV light (365 nm). Based on this unique property, spiropyran and lipid-polyethylene glycol (PEG) were mixed to fabricate photo-switching NPs, which shrank from around 100 nm to around 50 nm after exposure to UV light [47]. In an *in vivo* experiment applying a subcutaneous HT-1080 mouse tumor model, the tumor was irradiated (20 s, 1 W/cm^2) at 30 min post systemic administration of the NPs, and enhanced tissue penetration and antitumor effect was achieved. (iii) Light-generated heat, in particular photothermal heating of plasmonic NPs to break molecular bonds, such as DNA de-hybridization [48,49] or melting/disruption of polymer hydrogel [50] has been employed to release encapsulated cargo. (iv) Loss of membrane integrity by photo-oxidation [51] or by photothermal heating [38] has been used for release of cargo from endosomes/lysosomes. The details of strategies (iii) and (iv) will be further discussed in the sections below.

The different approaches require light excitation at different wavelengths. Strategies (i) and (ii) in general utilize UV-light, while visible and near infrared (NIR) light can be used in strategies (iii) and (iv). Irreversible photo-toxicity of UV-light on tissue at high intensities and its poor tissue penetration has limited *in vivo* application, and thus it is best applicable to regions of the body that can be directly illuminated, such as the eye or the skin [52]. Although two-photon excitation [53] and upconversion methods [54] which may convert NIR light excitation to photons in the UV have been utilized to avoid such disadvantage, in these cases high intensity and long irradiation times are often required [55]. Besides, lysosome disruption required for endosomal/lysosomal escape has, to our knowledge, not yet been reported by using UV-light. The utilization of visible and NIR light combining strategies (iii) and (iv) on the other hand would enable the release of cargo from both, the delivery vehicles and endosomes/lysosomes by photo-oxidative or photothermal strategies. The deep tissue penetration and reduced photo-damages of NIR light in the 800–1200 nm region make NIR laser highly attractive for remotely controlled release.

3.2. Photo-oxidation

Photo-oxidation involves either physically trapping or chemically conjugating a photosensitizer molecule or metal nanoclusters into the delivery vehicle. Both photosensitizer molecules and metal nanoclusters produce reactive oxygen species (ROS) (*e.g.*, singlet oxygen ($^1O_2$)) upon excitation with light. This can oxidize the matrix of the delivery vehicles, as well as the lysosome structure, and thus release the encapsulated cargo upon light irradiation into the cytosol. To prove the lysosomal disruption ability, Chen *et al.* efficiently incorporated Al (III) phthalocyanine chloride disulfonic acid (AlPcS2a), a potent photosensitizer, into polymer vehicles termed "PICsomes" [56]. Acridine orange emitted an intense red and green fluorescence (thus visualized as yellow) in acid organelles such as endosomes and lysosomes, while it emitted only green fluorescence in nuclei and cytosol. After endocytosis of AlPcS2a-PICsomes, lysosomal disruption was clearly observed after light irradiation of cells, as indicated by much decreased intracellular red fluorescence (Fig. 2). The photo-oxidation method has been applied in gene, drug, and protein delivery. Some prominent examples are described in the following.

Concerning gene delivery, several modes of photo-oxidation-based methods have been used. Two examples of three-layered polyplex micelles, which were prepared from the anionic dendrimer phthalocyanine, are shown in Fig. 3a,b. In these two systems, the positive polyplexes efficiently destabilized the lysosomes and enhanced *in vitro* and *in vivo* transfection efficiency 100-fold upon light (689 nm) irradiation [57,58]. A more sophisticated system is shown in Fig. 3c. In this approach an aggregation-induced emission (AIE) photosensitizer (TPECM) was conjugated with oligoethylenimine (800 Da) *via* a ROS cleavable aminoacrylate linker (AA). Excitation of the photosensitizer generated ROS, which then enabled simultaneous release and endo/lysosomal escape of DNA in a single irradiation process [51]. The ROS-sensitive cationic NPs self-assembled in aqueous solution and complexed DNA to form polyplexes. Upon light irradiation, the generated ROS disintegrated the high-molecular-weight polyethylenimine into low-molecular weight oligomer, which had low binding affinity to DNA, followed by DNA unpacking and release to the cytosol.

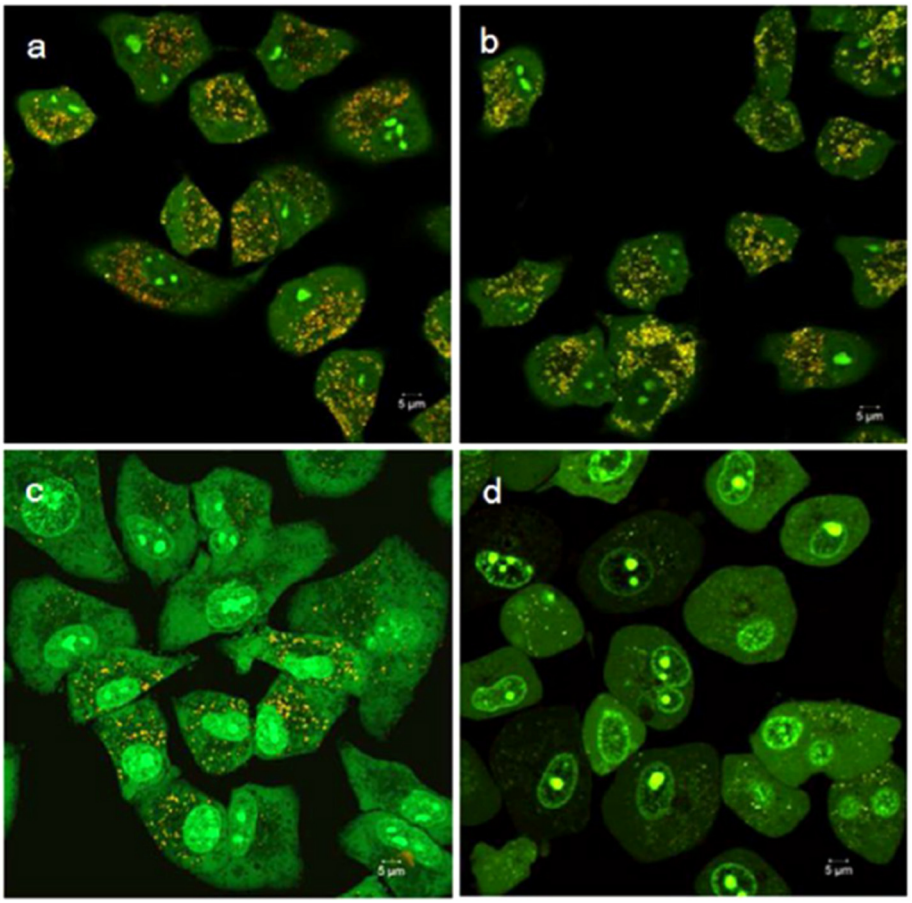

Fig. 2. Observation of lysosomal disruption of A549 cells induced by AlPcS2a-PICsomes. The cells were treated with (a) Phosphate-buffered saline (PBS) without irradiation, (b) light only, (c) AlPcS2a-PICsomes containing 0.05 μg/mL AlPcS2a, (d) AlPcS2a-PICsomes containing 0.2 μg/mL AlPcS2a, followed by 10 J/cm^2 laser application. The cells were further incubated with 6 μM acridine orange for 15 min before analysis with confocal laser scanning microscopy (CLSM). Adapted with permission from Chen *et al.* [56].

In respect to drug delivery, Rwei *et al.* synthesized a photosensitizer and incorporated tetrodotoxin, a ultrapotent local anesthetic drug into liposomes [59]. Irradiation at 730 nm triggered lipid peroxidation and uncaged the tetrodotoxin to block the sciatic nerve and achieve local anesthesia *in vivo*. Another permeability tunable liposomes doped with porphyrin-phospholipid has been demonstrated by Carter *et al* [60]. Light-triggered membrane permeabilization was enabled with liposomal inclusion of porphyrin-phospholipid, which was independent of bulk or nanoscale heating. In this work, the authors proved that following intratumoral injection, liposomes showed controlled release of an aminoglycoside antibiotic (gentamicin) and a fluorophore (sulforhodamine B). Following systemic administration, laser irradiation induced release of the anticancer drug doxorubicin in mouse xenografts suggested to be an excellent single-treatment antitumor therapy.

As a case of peptide delivery, Vasdekis *et al.* developed morphology switchable polymersomes with the photosensitizer ethyl eosin associated with the polymersome membrane (Fig. 4a) [61]. Light irradiation oxidatively increased the hydrophilicity of the hydrophobic block, which induced rapid polymersome rupture and reorganization into smaller diameter vesicles and micelles, leading to release of the encapsulated cargo molecules (Fig. 4b). As a demonstration of application, bone-marrow-derived murine dendritic cells were incubated with the polymersomes loaded with octapeptide ovalbumin major histocompatibility complex I (MHC I) epitope SIINFEKL. Antigen presentation was visualized with fluorescently tagged antibody specific for the SIINFEKL peptide/MHC I complex, and the kinetics were measured at single cell and even single complex level.

3.3. Photothermal release

Photothermal release of molecular cargo from a delivery vehicle can be achieved by different methods: (i) By embedding plasmonic NPs into the carrier matrix of delivery vehicles (such as polyelectrolyte shells), inside which the molecular cargo is embedded. Employed plasmonic NPs include silver NPs [62,63], gold sulfide NPs [64], spherical gold NPs [65,66], agglomerated gold NPs [7,41,67], gold nanorods [68,69] and gold nanostars [70], as also non-plasmonic NPs such as magnetite NPs [50] (Fig. 5a). Compared with nanorods and nanostars, the agglomeration of gold NPs is easy to prepare in the presence of high NaCl concentrations, but the huge variation in agglomerate size results in varied surface plasmon resonance peaks from batch to batch. The presence of gold NPs enhances the contrast of microcapsules in bright field microscopy, leading to darker capsules in the presence of higher density of gold NPs [70] and decreases the degradation of capsules [7,71]. (ii) By integrating a layer of graphene [72–74] or its derivatives [75] into carrier vehicles, such as multilayers capsules or liposomes. (iii) By incorporation of fluorescent probes with low quantum yield to the matrix of the delivery vehicles, *e.g.* IR-806 dye (maximum absorbance $\lambda_{max} = 806$ nm) to polymer capsules [63], DiD dye ($\lambda_{max} = 650$ nm) to liposomes [76], or indocyanine green ($\lambda_{max} = 800$ nm) to polymersomes [77]. (iv) By the formation of a plasmon resonant shell (*e.g.* gold) by *in situ* reduction of ionic metal ions such as gold onto the surface of the delivery vehicle, such as liposomes [78–80]. Microbubbles generated by photothermal excitation have been suggested being responsible for the breaking of the plasmonic shells [81], which leads to release of encapsulated molecules. (v) By conjugating the molecules to be released to host polymers

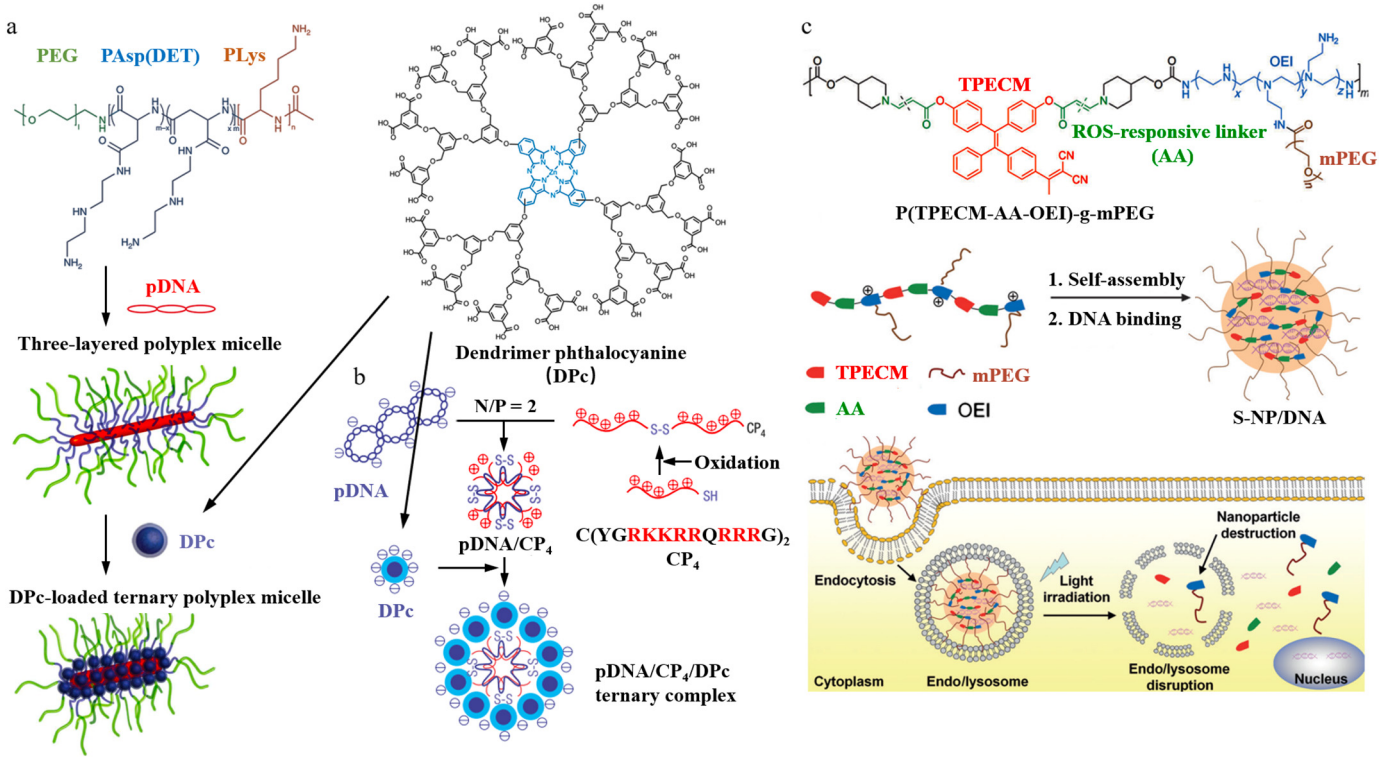

Fig. 3. Methods for photo-oxidation induced gene delivery. a) Scheme for preparing a three-layered polyplex micelle prepared from anionic dendrimer phthalocyanine and positive polyplex. Adapted with permission from Nomoto *et al.* [57]. b) Scheme for preparing a pDNA/CP4/DPc ternary complex. Adapted with permission from Nishiyama *et al.* [58]. c) NPs containing a light-triggered ROS generator and a ROS-cleavable linker on cationic polymers. Upon light irradiation, the generated ROS can concurrently destruct the endo/lysosomal membrane to facilitate the escape of the DNA vector and break the S-NPs to favor DNA unpacking, leading to DNA release for nuclear entry and transcription. Adapted with permission from Yuan *et al.* [51].

such as DNA [82–84] or proteins [82] *via* thermally labile linkage directly to the surface of plasmonic NPs.

As pointed out, apart from releasing cargo from the carrier vehicle, photothermal heating also needs to allow for endosomal escape for successful delivery of cargo to the cytosol. Different mechanisms have been suggested in this direction, though this phenomenon is not fully understood so far. Local heating may transiently open 100 to 200 nm pores for minutes [85], through which molecules may diffuse. Also, microbubble formation may be responsible for transient perforation of the membrane of endo/lysosome. As the carrier vehicles may be mechanically deformed upon photothermal heating (Fig. 5), also such mechanic effect may contribute to trigger transient rupture of endo/lysosomal membranes. The details of transient perforation are still subject to further research. Translocation to the cytosol has been demonstrated by the encapsulation of the pH-sensitive dye SNARF into polyelectrolyte capsules [7,38]. SNARF is a ratiometric pH indicator which has yellowish

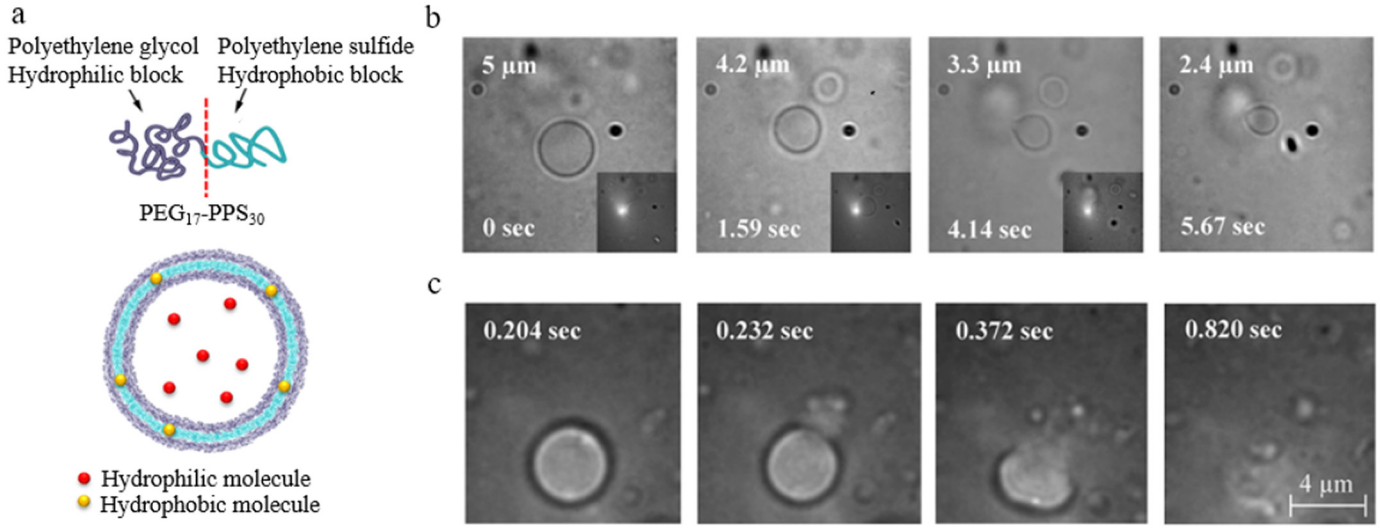

Fig. 4. Concept of optofluidic polymersome rupture. a) Chemical structure and scheme of PEG_{17}-b-PPS_{30} block copolymers and vesicles. PEG is the hydrophilic and polyphenylene sulfide (PPS) the hydrophobic block. b) Localized illumination of single vesicles for 1–2 s, which leads to the formation of smaller diameter vesicles. The vesicle diameters are indicated in each frame, while insets show the location of optical treatment at power densities of approximately 100 W/cm^2. c) Rupture of a single polymersome in a series of video microscopy frames. Illumination was at 500 W/cm^2. In subsequent optical treatments, a collimated excitation beam was employed, giving rise to lower excitation densities. Adapted with permission from Vasdekis *et al.* [61].

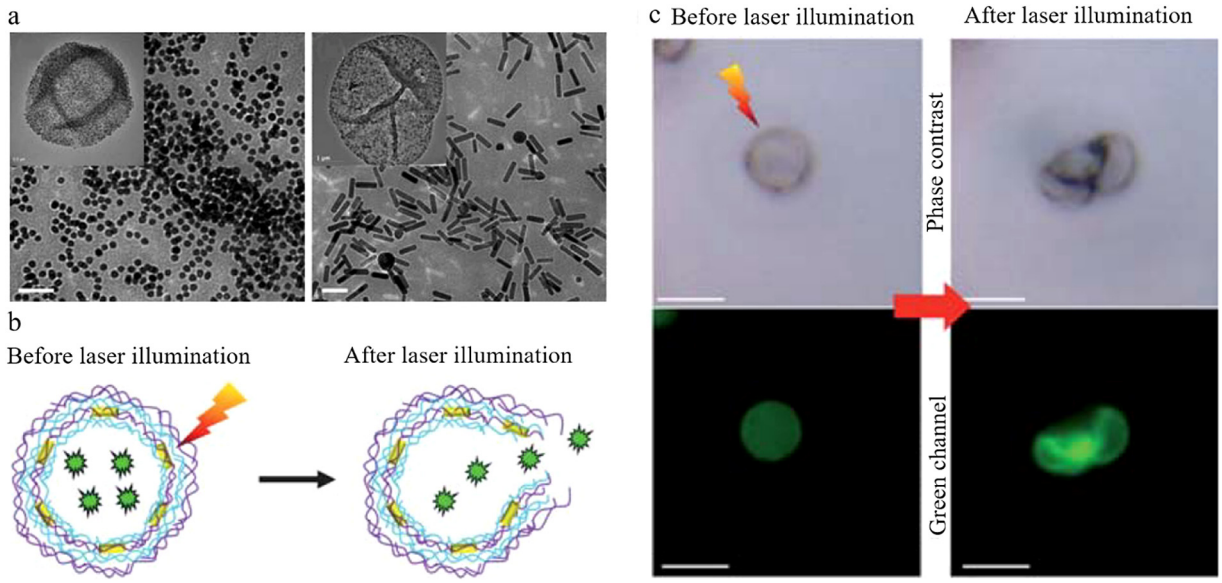

Fig. 5. Laser triggered opening of polyelectrolyte capsules with integrated plasmonic NPs in their shells. a) Typical transmission electron microscopy (TEM) images of spherical Au NPs (left) and rod-shaped Au NPs (right) as embedded inside the multilayer shell of hollow $(PSS/PAH)_4$ capsules. The insets show the single NP-modified capsules. The scale bars represent 50 nm. b,c) Laser-opening of capsules with rod-shaped Au NPs integrated in the capsule wall and encapsulated fluorescein isothiocyanate (FITC) labelled dextran. b) Schematic representation of the geometry of a capsule with green dextran as cargo (green stars) encapsulated inside the cavity and rod-shaped Au NPs (yellow rods) embedded in the wall. Laser irradiation of the Au NPs (left) leads to local heating of the NRs and subsequent rupture of the capsule wall (right). c) Effect of NIR laser irradiation (830 nm) of a single capsule with rod-shaped Au NPs in its wall and encapsulated FITC-dextran in its cavity. Before laser illumination the capsule retains the green cargo inside the cavity. After laser illumination the multilayer wall of the capsule is damaged (phase contrast) and partial release of the green cargo throughout the small pores of the wall is observed (green channel). The scale bars correspond to 5 μm. Adapted with permission from del Mercato *et al.* [69].

emission in acidic environments and red emission at alkaline pH. Upon light-mediated heating, capsules as well as the membrane of the surrounding endo/lysosomes were transiently opened, that SNARF was released from the acidic endo/lysosomal environment (yellow fluorescence of SNARF) to the neutral cytosol (red fluorescence of SNARF). Perforation of endo/lysosome was transient, as the rest of SNARF remaining trapped in acidic lysosomes showed yellow fluorescence (Fig. 6).

As with all delivery strategies, several processes are involved until encapsulated cargo is released into the cytosol, including membrane association of the delivery vehicles, their endocytosis and intracellular trafficking to endo/lysosomes, followed by release of the molecular cargo from the carrier vehicle and endo/lysosomal escape [29]. To quantitatively monitor all those steps still remains a challenge, in part due to the heterogeneity of the systems. In the following some applications of photothermal delivery of encapsulated molecules to the cytosol will be discussed. Hereby focus is given on polyelectrolyte capsules and liposomes as carrier vehicles. However, the reported concepts are rather general and would also apply to other carrier vehicles with integrated elements which can convert light to heat.

As first example live cell imaging based on intracellular immunostaining with impermeable fluorescence reporters is described. Fluorescent labeling of intracellular organelles for live cell imaging is challenging, as many fluorescent reporters, *e.g.* fluorescence-labelled antibodies targeting specific intracellular organelles can not penetrate the cell membrane. Thus, in general cells need to be fixed and perforated, which allows for entry of the fluorescent reporters, but exclude live cell imaging. In addition, single cell staining within a cell culture is almost impossible. Cells in principle may be transfected with fluorescent protein based reporters. Alternatively, the fluorescent reporters may be encapsulated into delivery vehicles, which then are endocytosed. Photothermal heating of plasmonic NPs in the delivery vehicles allows for release of the fluorescent reporters from the delivery vehicles as from endo/lysosomes [70]. In this example membrane-impermeable ATTO-488 labelled phalloidin, propidium iodide (PI), and 4,6-diamidino-2-phenylidole (DAPI) were encapsulated in PSS/PAH polyelectrolyte capsules decorated with gold stars. As shown in Fig. 7, multiplexed NIR opening of capsules loaded with different fluorophores enabled dual staining of the nuclei and F-actin within single cells in a controlled and specific manner. In a similar way, the

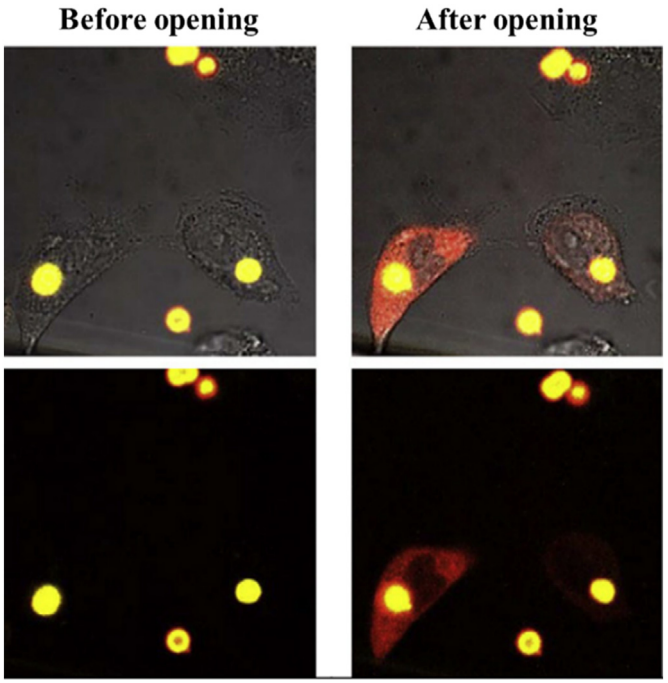

Before irradiation	After irradiation	
Capsule pH	**Capsule pH**	**Cytosol pH**
6.4 ± 0.3	7.1 ± 0.4	7.4 ± 0.4

Fig. 6. Capsule opening and subsequent cytosolic release of encapsulated 10 kDa SNARF-dextran upon light-mediated heating of Au NPs present in the capsule shell. Adapted with permission from Carregal-Romero *et al.* [38].

feasibility of photothermal release of encapsulated TO-PRO-3 iodide into cells with the purpose of nucleus staining has also been demonstrated using plasmonic liposomes as carrier vehicles [86]. While transient endo/lysosome permeation *via* photothermal heating has been demonstrated to be tolerated by cells without instantaneous loss in cell viability [64], there are clear side effects, such as the triggering of Ca transients [87,88]. While "life" staining thus in principle is possible, it always has to be analyzed if unwanted side effects upon photothermal heating may interfere with experiments.

As second example we want to highlight the controlled triggering of cytosolic reactions/processes. The delivery of molecular reactants into the cytosol of cells typically involved endocytosis, which is a statistical process, and translocation to the cytosol by endo/lysosomal escape. In this way it is not clear at which point of time reagents enter the cytosol and the reaction would start, which complicates recording kinetics. In case reagent are encapsulated, they are endocytosed together with their carrier vehicle. Only after a light trigger, instantaneous release of the reagent to the cytosol would happen, clearly connecting the starting point of the intracellular reaction with the light trigger. This has been demonstrated with polyelectrolyte capsule with plasmonic NPs in their wall, and encapsulated reagents, non-fluorescent substrate ELF97, and alkaline phosphatase, both in different capsules [41]. Sequentially light triggered opening of individual capsules within one cell brought ELF97 and alkaline phosphatase to be both present in the cytosol. Cleavage of the phosphate group of ELF97 by alkaline phosphatase enzymes converted ELF97 into green fluorescent ELF97 alcohol. After the opening of the first capsule, the enzyme or substrate was released into the cytosol. Opening the second capsule with the complementary cargo led to the enzymatic reaction, *i.e.* generation of insoluble ELF97 alcohol, which precipitated close to the second opened capsule. The same platform was employed to release encapsulated mRNA encoding green fluorescent protein (GFP) to the cytosol. This allowed to record the reaction kinetics of GFP production from the time when mRNA has release into the cytosol, with the light trigger defining the time point zero [41]. Also complex biological reactions could be triggered, such as cell surface antigen presentation. Major histocompatibility complex (MHC) class I molecules are transmembrane receptors which can travel to the cell surface after binding to specific intracellular peptides of 8–10 amino acids in length [89]. After a virus-derived peptide is complexed with MHC class I at the cell surface, cytotoxic T lymphocytes can recognize this structure and will kill those antigen presenting cells [90]. Palankar *et al.* encapsulated a fluorescence-labelled Ser-Ile-Ile-Asn-Phe-Glu-Lys-Leu peptide, a specific ligand for MHC class molecule H-$2K^b$, into (PSS/poly(diallyldimethylammoniumchloride) (PDADMAC))$_4$ capsules decorated with gold NPs [66]. After laser exposure, the capsules opened and the peptide, efficiently bound to the H-$2K^b$ and elicited their cell surface transport to present antigen.

Also intercellular signaling was investigated. In general, when studying cell-cell communications, evaluation of the propagation signal or response from a stimulated cell to the surrounding cells needs to be analyzed. In that context, light-triggered opening of individual carrier vehicles can generate local release which stimulates individual cells, allowing to measure signal spread to surrounding cells. Inositol trisphosphate (IP3), an endogenous cell signaling second messenger, has been encapsulated in liposomes modified with plasmonic NPs to allow for light-triggered intracellular calcium increase in the irradiated cells [80,92]. Orsinger *et al.* encapsulated either IP3, or adenophostin A (AdA), a potent analogue of IP3, into 100 nm plasmonic liposomes. The release of IP3 or AdA efficiently initiated calcium release from intracellular stores, followed by intercellular calcium wave propagation (Fig. 8a) [78]. While the previous examples, were releasing encapsulated cargo from internalized delivery vehicles was used to trigger intracellular reactions, release can also be applied extracellularly, as again demonstrated for light-triggered intercellular calcium signaling. Raise

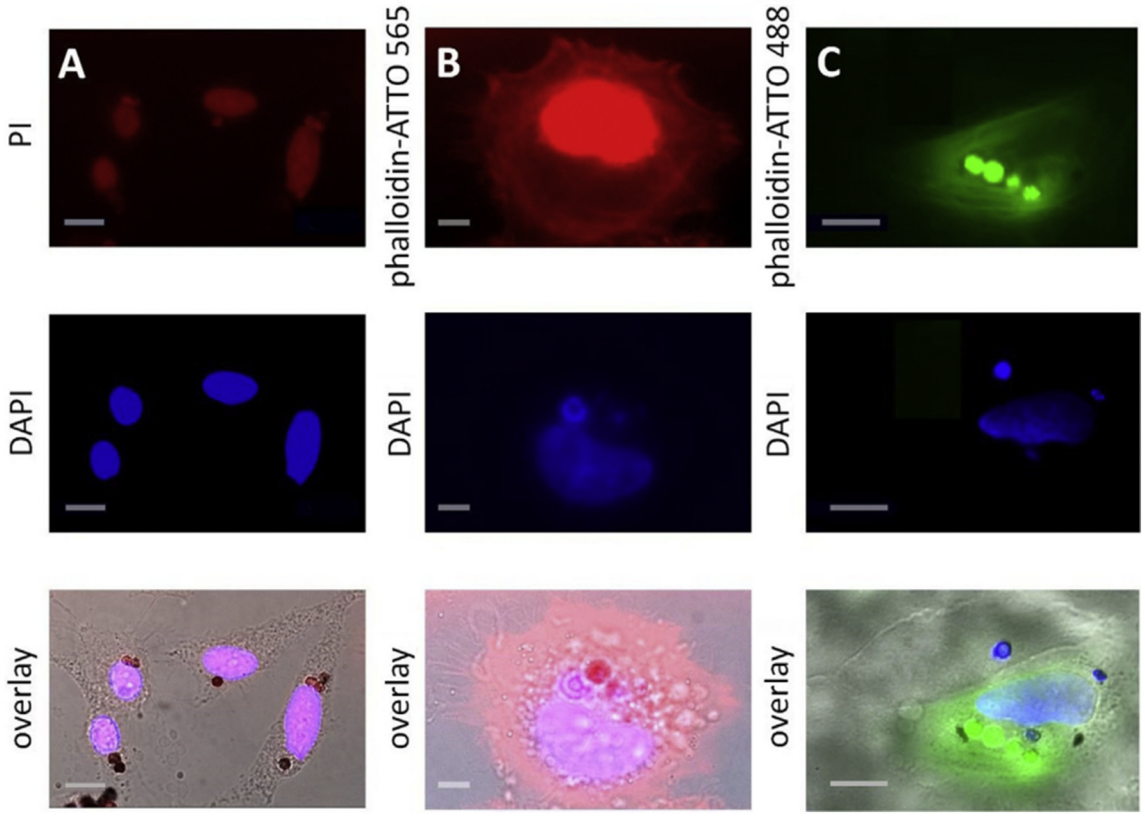

Fig. 7. Multiplexed intracellular opening of capsules with different encapsulated fluorescent reporters. a) Combination of propidium iodide (PI) and (4′,6-diamidino-2-phenylindole) (DAPI). The sale bars indicate 20 μm. b) Combination of phalloidin-ATTO-565 and DAPI. The scale bars correspond to 10 μm. c) Combination of phalloidin-ATTO-488 and DAPI. The scale indicate 20 μm. Adapted with permission from Kantner *et al.* [70].

in intracellular calcium concentration increase can be achieved by extracellular release of CCK8. CCK8, a hydrophilic peptide derivative agonist of the endogenous cholecystokinin ligand, was encapsulated into the liposomes modified with plasmonic NPs (Fig. 8b) [91]. After extracellular opening of the liposomes, CCK8 was released in proximity to cells and activated the membrane-bound CCK2 G-protein-coupled receptor, which resulted in spikes in intracellular calcium concentration. These experiments demonstrate that light triggered release *via* photothermal heating offers the advantage to record the kinetics of intracellular processes independently from cellular uptake and carrier system degradation. Light activated all-trans retinoic acid (atRA) release has also been demonstrated to induce the expression of RARE element, followed by driving transcription of firefly luciferase gene in a NB4-RARE report cell line [22]. The atRA was conjugated to PEI *via* a photocleavable ortho-nitrobenzyl-based linker to form PEI-atTA NPs. Once inside cells, the UV activation efficiently released the atRA to induce atRA signaling and improved luciferase expression.

Intracellular signaling has been also controlled *in vivo* [93]. It has been demonstrated that Wnt signaling in hydra can be turned-on by light-triggered release of alsterpaullone. Alsterpaullone is an intracellular modulator of the Wnt pathway and was encapsulated in polyelectrolyte microcapsules modified with Au NPs in their walls, which were fed to hydra [71]. Light-mediated capsule opening released alsterpaulone. While in the "on" state, the released alsterpaulone inhibits the GSK3β kinase and stabilized β-cat is translocated into the nucleus to active Wnt downstream genes. Accordingly, the hydra presented ectopic tentacles through the column (Fig. 9) [71].

As third example we discuss drug and gene delivery for anticancer therapy. In the context of the design of stimuli-controlled vehicles, drug and gene delivery systems are one of the most widely investigated applications. For instance, therapeutics against breast cancer, for which no effective standard therapy and proprietary drugs have been approved, have been developed by Su *et al.* [77]. The authors designed polymeric carrier vehicles loaded with indocyanine green (ICG), paclitaxel (PTX), and survivin siRNA (Fig. 10a). Light-triggered photothermal heating of ICG increased the temperature above the lower critical solution temperature (LCST) of the polymer matrix, causing deformation of its core-shell structure and release of PTX and siRNA to the target site. This system was reported to exert remarkable antitumor efficacy at low drug dose and low side effects [77]. Also melting of complementary DNA at temperatures above the melting temperature (T_m) can be used as a strategy for controlled opening of delivery vehicles. The melting temperature can be tailored by the type and length of oligonucleotides. For instance, the theoretical melting temperature of a 12 base-pair sequence contains an equal number of 4 different nucleotides, namely AAATTTCCCGGG, is $T_m = 50.0$ °C, which can be readily achieved by photothermal heating. As an example, double-stranded DNA was tethered into mesoporous silica NPs to encapsulate the anticancer drug doxorubicin (DOX) [48]. Photothermal heating of integrated rod-shaped Au NPs dehybridized the DNA duplexes and allowed for the release of DOX and oligonucleotides. The oligonucleotides were further designed as GFP-interfering siRNA, which provided additional gene delivery (Fig. 10b) and showed efficient GFP silencing in HeLa GFP cells [48]. Another straightforward design was achieved by Xiao *et al.* who designed a DNA-based platform with the ability to release therapeutics (DOX) (Fig. 10c) with antitumor efficacy in KB and HeLa subcutaneous tumor models (Fig. 10c) [49]. Another mechanism for light-induced siRNA release from Au NP surfaces is the cleavage of the gold-sulfur bond [94]. Besides these NPs, microcapsules functionalized with rod-shaped Au NPs have also been explored for *in vivo* antitumor testing [95]. The capsules were covered with fluidic lipid bilayers to decrease the wall permeability and retain the encapsulated DOX. After intratumoral injection, the NIR irradiation of the tumor site rapidly released the DOX to inhibit tumor growth and metastases.

4. Alternating magnetic field-triggered release

Magnetic NPs have been extensively investigated as heat mediators for magnetic hyperthermia under an alternating magnetic field (AMF) [96–99]. In a similar way to photothermal release, heating of magnetic NPs also might be used for the disintegration of carrier vehicles and release of encapsulated cargo molecules [17], leading to magnetothermal release.

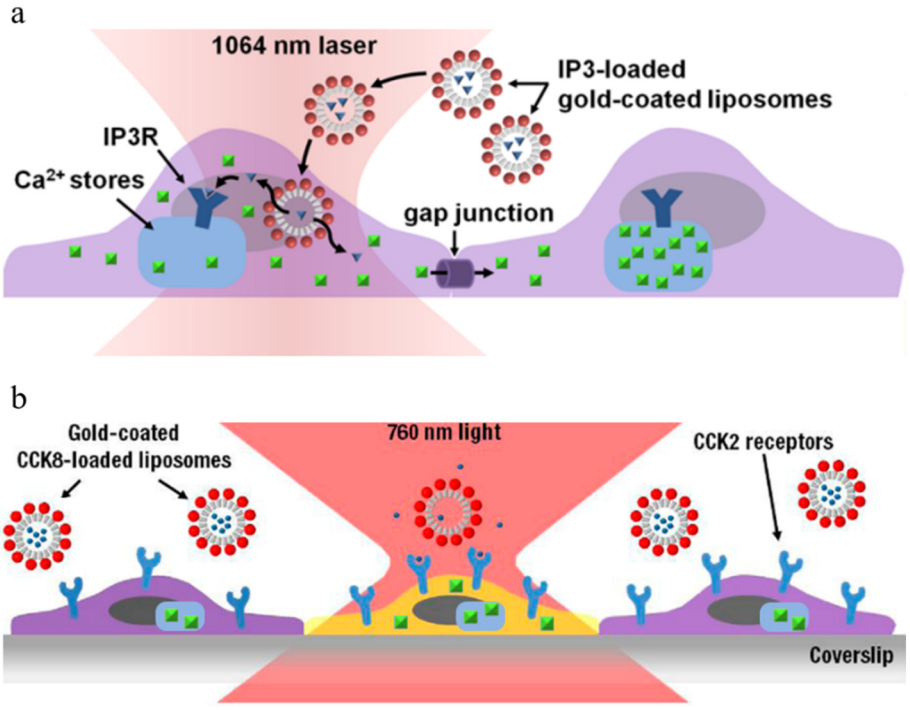

Fig. 8. Schematic drawing of the light-induced intracellular increase of Ca^{2+} after release of encapsulated cargo a) from internalized plasmonic liposomes and b) from extracellular plasmonic liposomes. Adapted with permission from a) Orsinger et at [78] and b) Leung *et al.* [91].

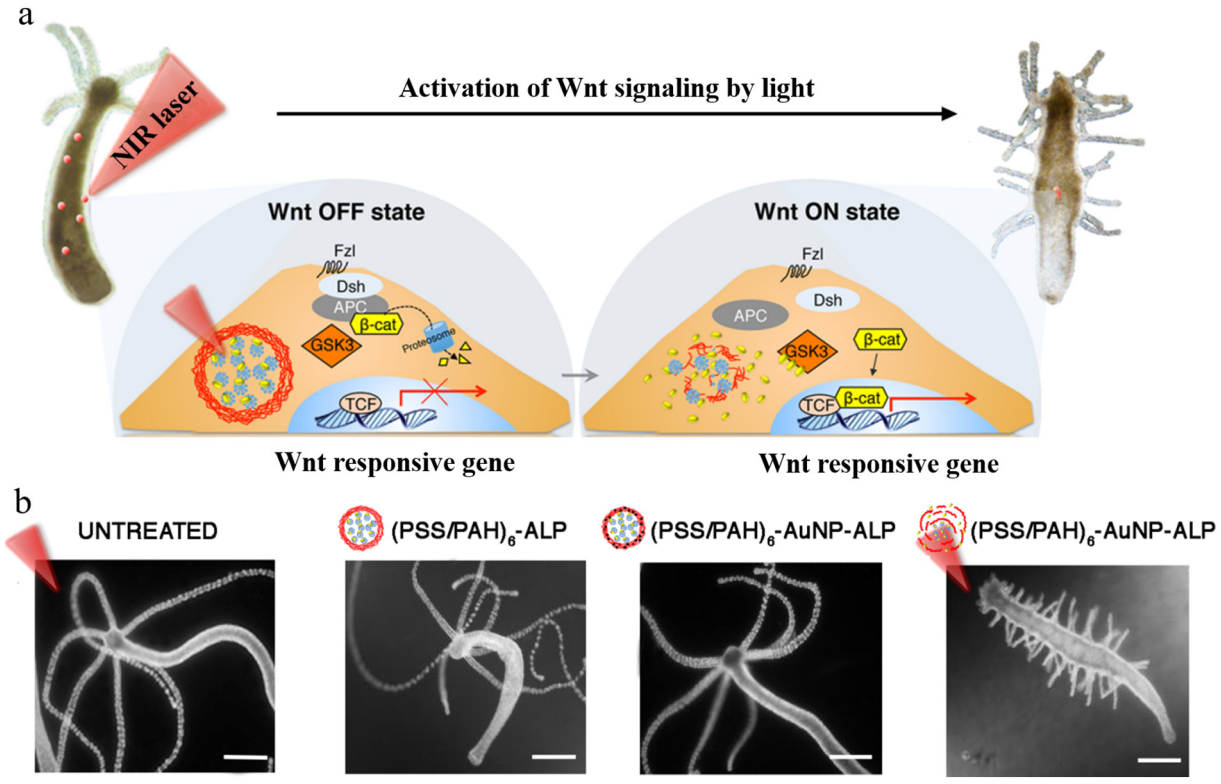

Fig. 9. NIR-triggered activation of the Wnt signaling pathway. a) Scheme of Wnt signaling pathway activation by released alsterpaullone. Following NIR irradiation of $(PSS/PAH)_6$-Au NP-alsterpaullone capsules internalized by hydra, the Wnt molecular cascade is switched on and the hydra presented ectopic tentacles through the column. b) Morphologies of hydra after different treatment. Adapted with permission from Ambrosone *et al.* [71].

Magnetic NPs can generate heat under an AMF due to the hysteresis loss and Néel relaxation [100]. AMF-triggered release can be realized by different geometries: (i) Magnetic NPs such as iron oxide NPs or Co@Au NPs can be integrated into delivery vehicles which encapsulate the molecular cargo (such as calcein [101], phenol red [101], pyranine [101], doxorubicin [102], dye-labelled dextran [17,102,103]), *e.g.* to the walls of polyelectrolyte capsules [17,102,103], liposome/copolymer hybrids [104], polyelectrolyte capsules coated with lipids [101] and polymersomes [105]. (ii) Molecular cargo such as dyes (*e.g.* tetramethylrhodamine [106]) or anticancer drugs can be conjugated to magnetic NPs *via* thermo-sensitive molecules, such as azobis[N-(2-carboxyethyl)-2-methylpropionamidine] [107] or a reversible retro Diels-Alder reaction between a furan group and *N*-methylmaleimide [106]. (iii) Molecular cargo may be encapsulated by a thermosensitive hydrogel forming a shell around magnetic NPs [108].

Based on the different geometries different mechanisms have been applied to the AMF-triggered release payload: (i) Rupture of the shell of polymeric delivery vehicles. Authors claim that both magneto-thermal effects and mechanical vibration and motion led to shell structures to form 50–100 nm nanocavities (Fig. 11a), and their continuous enlargement resulted in final rupture of the shell (Fig. 11b,c) and burst release of payload (Fig. 11d) [102]. (ii) Katagiri *et al.* suggest that the phase transition of thermosensitive copolymers doped in liposomes [104] or lipid coats on polyelectrolyte capsules [101] is responsive for magneto-thermal release, rather than the rupture of the capsules. (iii) When the antitumor drug *e.g.* tamoxifen was loaded to the inner hydrophobic cavity of β-cyclodextrin, which was linked to 12 nm ironoxide NPs, the temperature in response to the AMF generated heat depressed the hydrophobic interaction and accelerated drug release [109]. (iv) The thermosensitive polymer poly(N-isopropylacrylamide) (PNIPAAm) formed a hydrogel shell around the micron-sized iron oxide particles. The heat generated upon AMF exposure increased the temperature above the LCST of PNIPAAm, which made the hydrogel shell collapse and resulted in release of encapsulated drugs [108]. Similarly, yolk/shell capsules were prepared from magnetic iron oxide NPs as the core, a thermal sensitive polymer PEO-PP-PEO (Pluronic F68), and silica shell. Above the critical micelle temperature, the core shrunk and the size decreased more than 10 times, causing shell destruction and collapse and subsequent release of encapsulated ibuprofen [110]. (v) In self-assembled polyvinyl alcohol (PVA)-iron oxide NP/silica core-shell carrier vehicles, magnetic-induced heating caused dissolution and increased flexibility of PVA, which gave rise to nanocavity formation and core disintegration [111].

While AFM-mediated heating of magnetic NPs is highly established for hyperthermia applications, release of encapsulated cargo molecules upon magnetothermal heating is less reported in literature, particularly when compared with various applications of light-triggered carrier vehicle opening. Most reports involving in AMF-responsive carrier vehicles rather remain at the proof of principle level, sometimes even without further application in cells. Some interesting concepts of molecular release upon magnetothermal heating are presented in the following.

One concern of AMF application is that hyperthermia causes irreversible damage in cells and tissues at temperature in the range of 42–45 °C [112]. Hence, it is essential to measure the local and nearby temperature of magnetic NPs upon magnetothermal heating. To address this issue, Riedinger *et al.* have developed a direct method to quantify the local temperature profile on the surface of magnetic NPs exposed to an AMF with a subnanometer resolution [107]. The dye fluoresceineamine was conjugated to thermolabile azo-linkers at the surface of magnetic NPs, using PEG-spacers of distinct molecular weights. An increase in temperature accelerated cleavage of the azo group thus released the dye from the iron oxide NPs (Fig. 12a). The released dye was separated by ultracentrifugation, and its fluorescence intensity reflected changes in temperature. Significant local heating at distances occurred only within 0.5 nm from the NP surface where the temperature increased to 45 °C [107], while the increase in temperature decayed almost to zero at distances longer than 4–5 nm (Fig. 12b).

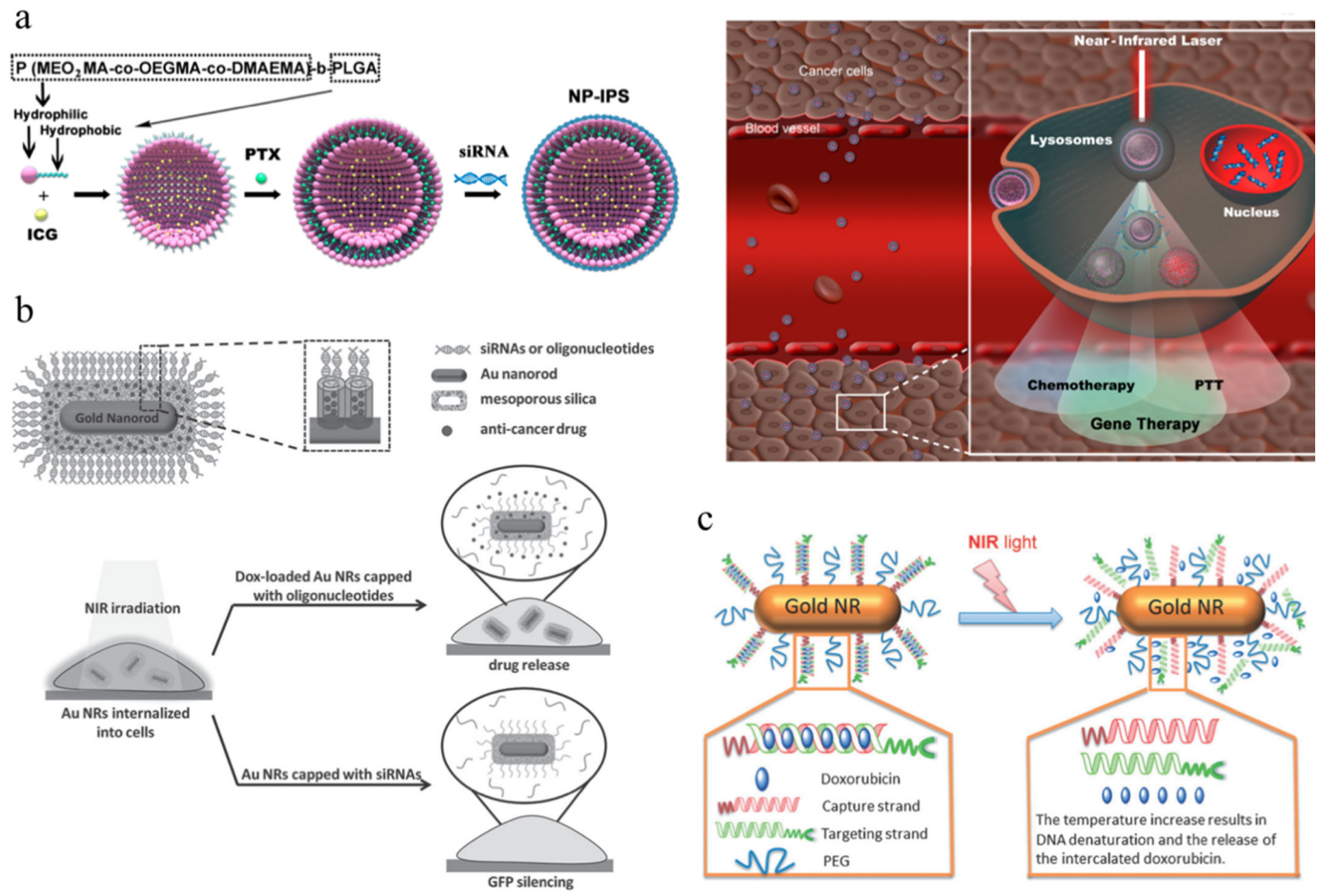

Fig. 10. Light-induced drug and gene delivery for anticancer therapy. a) Polymersomes containing ICG, PTX, and siRNA for the combination of thermotherapy, chemotherapy, and gene therapy. b,c) Rod-shaped Au NP based drug delivery system *via* melting of complementary DNA upon NIR stimuli. b) Delivery of DOX or siRNA through dehybridization of DNA tethered to mesoporous silica shells with Au NPs as inside core. c) Delivery of DOX through dehybridization of DNA conjugated to the surface of Au NPs. Adapted with permission from a) *Su et al.* [77], b) Chang *et al* [48], and c) Xiao *et al* [49].

Furthermore, this system was used for drug delivery through replacing the dye by doxorubicin for cancer treatment on KB cancer cells (Fig. 12c). A similar thermometer was also reported by Dias *et al.* [113].

Also melting of complementary DNA can be achieved in magneto-thermal systems [114], similar to the one achieved by light-triggering plasmonic NPs as discussed above. In this case, a single strand DNA of 12, 18 or 24 bases linked to a fluorophore was hybridized to a complementary 30 bases DNA, which was conjugated to dextran-coated iron oxide NPs (Fig. 13a). The matrigel plugin containing NPs was subcutaneously implanted to mimic a tumor model (Fig. 13b). Application of AMFs (400 kHz, 1.25 kW) caused fluorophore release and penetration far into the nearby tissue, while no fluorescence outside implant tissue was observed in unexposed controls (Fig. 13c,d) [114].

Magnetothermal heating has been also employed for the opening of molecular gates in mesoporous silica nanoparticles (MSNs). MSNs have attracted wide-spread interest as functional materials due to their low toxicity and high drug loading capacity. Additional nanogates may be applied for capping the surface pores of MSNs to prevent undesirable release of encapsulated cargo molecules. To achieve this, magnetic NPs can be used either as the nanogate on the MSNs' surface or can be encapsulated inside the MSNs to trigger the opening of other nanogates for on-demand drug release. Ruiz-Hernandez *et al.* [115] designed DNA/magnetic NPs conjugates as nanogates to cap the pores of MSNs upon DNA hybridization (Fig. 14a). Local heat generated by an AMF (100 kHz, 24 $kA \cdot m^{-1}$) increased the temperature (42–47 °C), enabling the melting of double-stranded DNA. This gave rise to uncapping of the MSNs and the subsequent release of an encapsulated model drug. Thomas *et al.* [116] developed another magnetic field responsive nanogate opening system. Zn-doped Fe_3O_4 NPs were loaded into MSNs and thermal responsive cucurbit[6]uril was electrostatically bound to the molecular thread on the surface as nanogate (Fig. 14b). The nanogate was non-self-opening in biological systems, but it could be opened at increased temperature. Doxorubicin-loaded MSNs displayed significant cancer cell killing efficiency after exposure to an AMF (500 kHz, 37.4 $kA \cdot m^{-1}$). The surface pores in the MSNs were further blocked by a crosslinked PEG shell functionalized with azo bonds (Fig. 14c) [117] or with a lipid bilayer (Fig. 14d) [118]. Again, exposure to an AMF induced burst release of the encapsulated drugs.

Last but not least direct encapsulation was demonstrated [17,119]. A double emulsion method has been applied for encapsulating FITC-labelled DNA (2.7 kbasepairs) and magnetic NPs into the cavity of hydrophilic capsules [119]. After endocytosed by MCF-7 cells, the cells were exposed to an AMF (50 kHz, 2.5 $kA \cdot m^{-1}$) for 2 min. Local heating increased the permeability of the hydrophobic shell and enhanced the diffusion rate of DNA. The intracellular fluorescence intensity increased 5–6 fold, which was caused by the reduced quenching effects after DNA escaped from the confined space inside the capsules and increased local pH after endo/lysosomal escape.

5. Photo- *versus* magneto-thermal heating for triggered release of encapsulated molecules

Light and AMFs stimuli are based on the excitation of plasmonic and magnetic NPs through an electromagnetic field, but at different

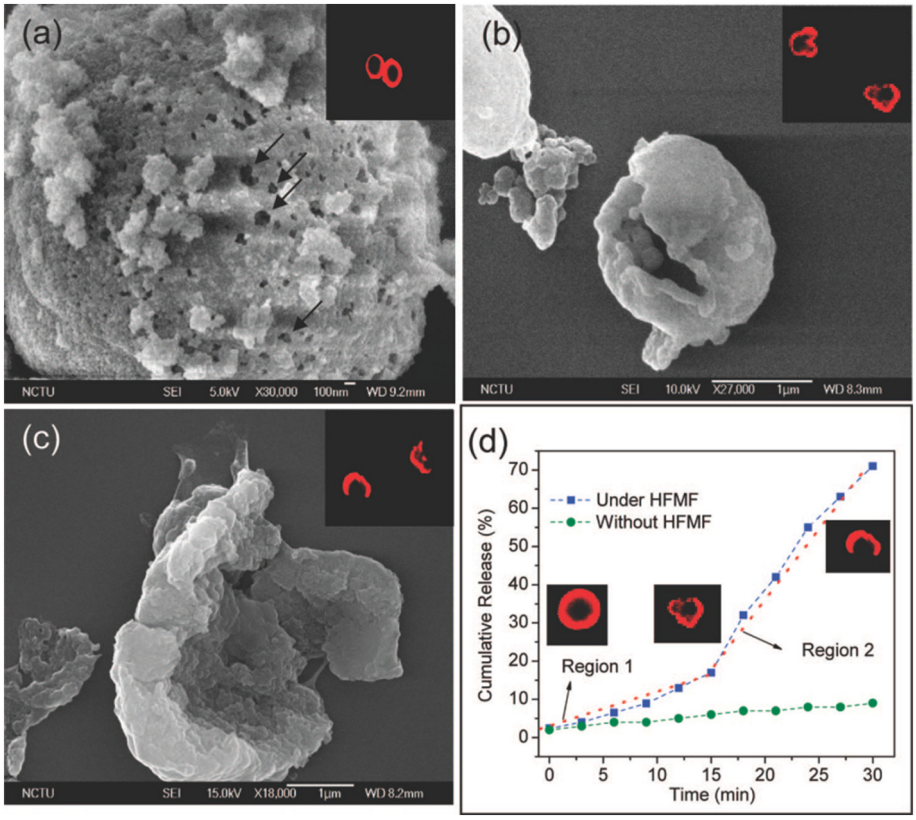

Fig. 11. Scanning electron microscopy (SEM) and CLSM images of $(Fe_3O_4$ NP/PAH$)_4$ capsules after an AMF treatment for a) 10 min, b) 15 min, and c) 30 min. After 10 min stimulus, a certain amount of nanocavities, 50–100 nm in size, appeared on the surface of the capsules. Upon further increasing the AMF stimulus to 30 min, the capsule walls were ruptured to a large extent. d) The drug release behavior and morphologies of $(Fe_3O_4$ NP/PAH$)_4$ capsules under continuous AMF irradiation. Adapted with permission from Hu *et al.* [102].

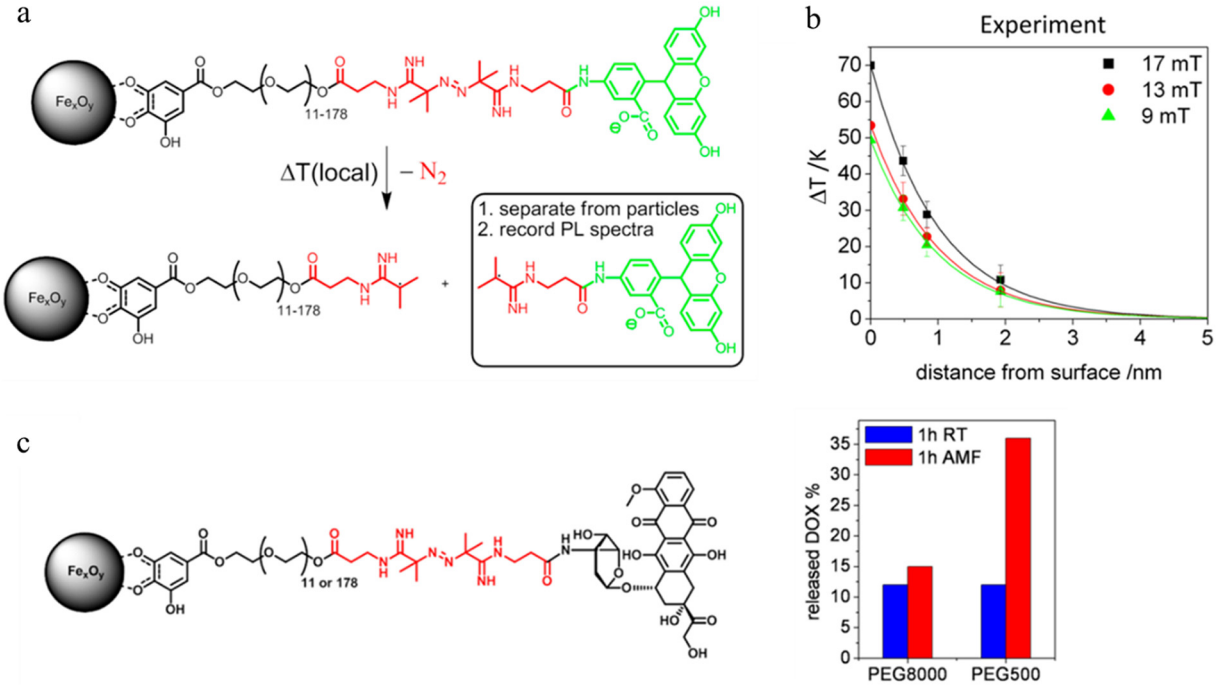

Fig. 12. Subnanometer local temperature probing and drug delivery. a) A sketch of iron oxide nanoparticles bearing fluoresceinamine connected through VA057 azo molecules to the tails of PEG spacers of different molecular weights. Increase in temperature resulted in accelerated cleavage of the azo group and release of the dye from the NPs. b) Experimental temperature gradients for all field amplitudes: significant local-to-global temperature differences were found at distances shorter than 3 nm. c) A sketch of iron oxide NPs bearing DOX which was covalently linked through VA057 azo to PEG spacers of two different molecular weights (500 and 8000 Da). The release profile of DOX from samples exposed for 1 h at room temperature to AMF irradiation (334.5 kHz, 17 mT) is shown. Adapted with permission from Riedinger *et al.*. [107].

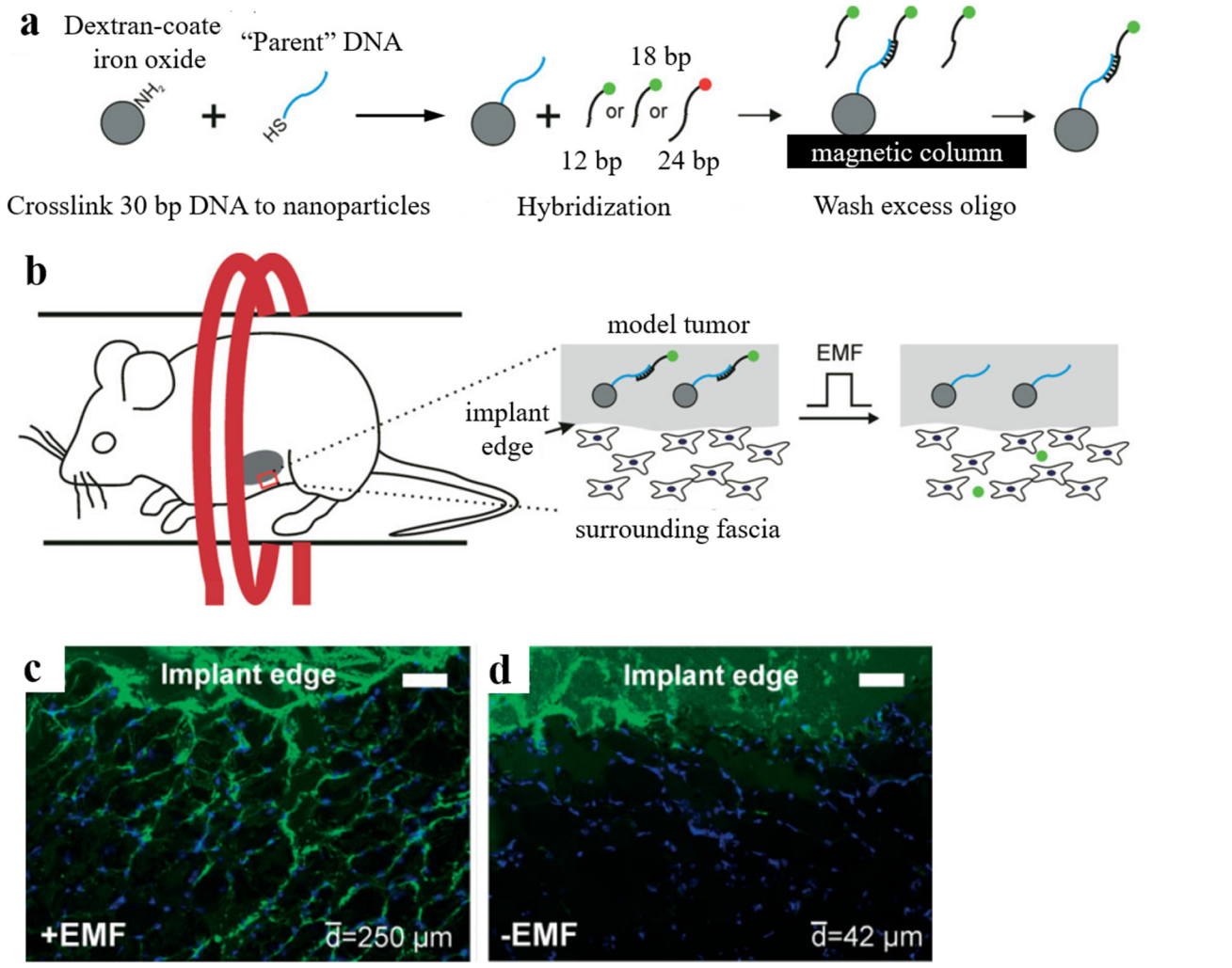

Fig. 13. Melting of complementary DNA by AMF-generated heat on the surface of magnetic NPs. a) A 30 base-pair "parent" strand was covalently linked to dextran-coated iron oxide NPs, allowing a fluorescence-labelled DNA complement (of 12, 18, or 24 bases) to hybridize. b) Remotely triggered release from NPs *in vivo*. The NPs were mixed with a matrigel and injected subcutaneously near the posterior mammary fat pad of mice, forming model tumors. c) Application of AMFs to the implants resulted in release of model drugs and penetration into nearby tissue. Adapted with permission from Derfus *et al* [114].

frequencies (note that AMFs are also a special form of electromagnetic fields). The frequency of light for photo-oxidation or photothermal heating is in the visible and NIR range, while the frequency of AMFs is in the radiofrequency range. AMFs are much less absorbed by tissue than light, and thus penetrate much deeper. For instance, 99% of magnetic fields at 400 kHz can penetrate 15 cm of tissue [120]. Furthermore, ultraviolet-visible light (less than 600 nm) has poor penetration ability (~2 mm in depth) due to strong scattering in soft tissue. Wavelengths in the NIR window permit deeper penetration, however, the intensity of light (800–860 nm) after penetrating 8 mm through rat skin still is reduced to 5% of its original level [23]. In general, light-triggered vehicle opening usually occurs within few seconds, while in the case of AMF to achieve similar effects the desired time may be higher from minutes and hours. In general, it is very easy to generate high temperatures upon photothermal heating of plasmonic NPs, which for example routinely allows for water evaporation [67]. "Overheating" thus becomes a potential problem. In contrast, typically lower increase in temperature is achieved by magnetothermal heating of magnetic NPs when applied with excitation parameters compatible with requirements of organisms. Light can be readily focused to as small as few microns, enabling the manipulation on a single-capsule level [38], which so far has not been demonstrated for AMFs. Light irradiation of plasmonic NPs can de-stabilize surrounding endo/lysosomal membrane *via* photo-oxidation or photothermal effects, whereas to our knowledge there is still no direct evidence in this direction in the case of AMF application. Beside the promising use of photo- and magneto-thermal heating as external triggers for biomedical application, additional studies are needed to address their potential benefits, efficiency and safety. Major improvements would be needed to considered issues regarding tissue-penetration depth with higher specificity, while avoiding any undesirable damage to the surrounded healthy tissues. A summary of the different characteristics of both methodologies is given in Table 1.

As discussed above, light- and AMF-triggered release have advantages and disadvantages and the better choice will depend on the particular application. In this direction we want to mention one additional example, which is not based on the release of drugs, but on direct killing of bacteria by light- [121] or AMF-induced [122] heat. Hyperthermia can be caused by photothermal [123] and by magnetothermal heating [124]. Magnetothermal heating has been used to destroy bacterial films on implants [121]. Here the advantage is, that the AMF may penetrate into tissue and this methodology could be applied *in vivo*. On the other hand, as implants may include magnetic impurities, limits in focusing might results in unwanted heating of the whole implant. Photothermal heating on the other hand can be better focused, but application would be limited to implants close to the skin due to limited penetration depth. Having both options at hand will allow for finding the better methodology for each respective application.

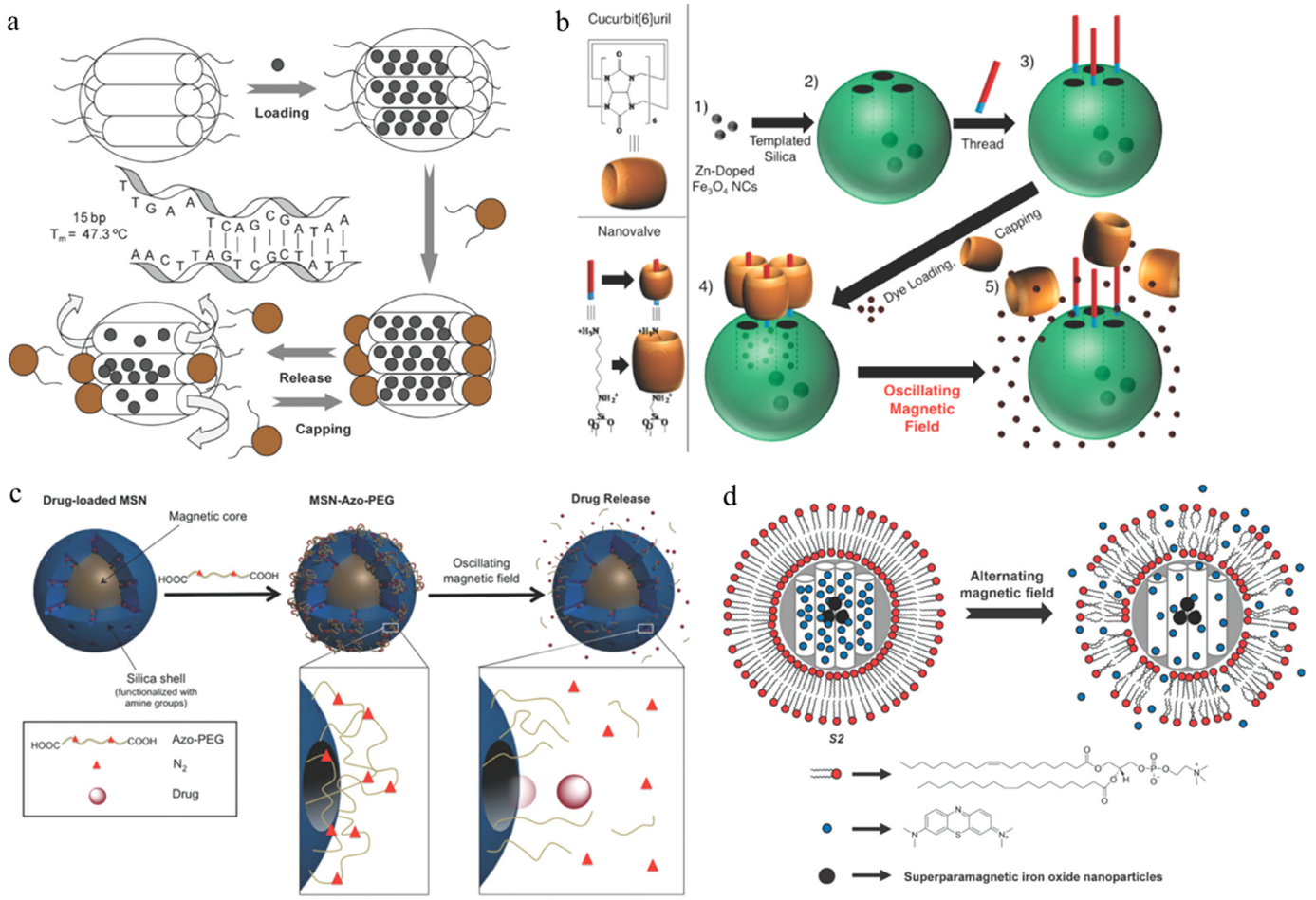

Fig. 14. AFM triggered nanogates opening and cargo release in mesoporous silica nanoparticles (MSNs) containing magnetic NPs. a) DNA/magnetic NP conjugates as the nanogate. b) Cucurbit[6]uril based nanogate. c) Crosslinked poly(ethylene glycol) (PEG) shell functionalized with azo bonds as the nanogate. d) Lipid layer coating as the nanogate. Adapted with permission from a) Ruiz-Hernandez *et al.* [115], b) Thomas *et al.* [116], c) Saint-Cricq *et al.* [117], and d) Bringas *et al.* [118].

6. Outlook

Today a variety of hybrid nanocomposite delivery vehicles are designed with distinctive physicochemical characteristics including size, surface functionalization, low toxicity, *etc.* Specific delivery of a compound to the desired site is crucial for improving the efficacy of treatment, while minimizing possible toxic effects. Materials allowing for drug release on demand would be helpful towards temporal control of the local concentration of the pharmaceutical compound. Stimuli responsive systems benefit from the possibility of switching the release of the compound in a controlled manner, representing an attractive concept for advanced drug delivery systems. There are a variety of stimuli that could be applied to trigger cargo release from delivery vehicles. The design of remotely controlled vehicles by light and AMFs represents an interesting platform in this direction, as light and AFMs are triggers which can be externally controlled [18], in contrast endogenous triggers such as redox potential or pH. Light-triggered release has also been demonstrated to offer solutions for the general problem of endo/lysosomal escape.

While in general stimulus response therapies may offer superior specificity and reduce toxicity in comparison to traditional or standard therapies (*e.g.* chemotherapy for cancer), only a limited number of studies have shown positive *in vivo* outcomes so far, and even fewer have been translated to clinical trials. Several shortcomings and challenges

Table 1
Overview summarizing the main advantages and disadvantages of photo- and magnetothermal heating for triggered release of encapsulated molecules.

Property	Photo-trigger		Magnetic-Trigger	Reference
	UV-Light	NIR	Radiofrequencies	
	Characteristics	Characteristics	Characteristics	
Ability to disrupt chemical structures	High	Moderate	Low	[19–22,25,42–45]
Tissue penetration ability	Poor	Good	Very good	[23,52,54,55,114]
Possible toxicity	High	Low	Very low	[24,54,55]
Lateral damage to intracellular compartments	High: surrounding endo/lysosomal membranes can be destabilized *via* photo-oxidation or photothermal effects		Very low	[23,24]
Heat generation	Very fast Overheating is a drawback		Slow process. No danger of overheating	[38,48–50,108,115]
Focus	Focusing micrometer size areas is easily possible		Focusing to smaller areas is difficult	[38]

are still needed to be addressed for a potential successful development of those therapies towards clinical applications [125]. Some major concerns are highlighted in the following. In general, for the suitable development of stimulus-controlled release materials, it is essential to understand and illustrate the mechanisms involved in the release procedure. This has been shown to large parts for the release of encapsulated molecules from delivery vehicles upon photo- or magnetothermal heating. However, accompanying endo/lysosomal release has not yet been fully understood and optimization in respect to efficiency is needed. Avoiding side effects, as toxicity of the delivery vehicles or damage due to the actual release process is crucial. Therefore, biocompatibility studies of the carriers itself as well as concerning the source of the stimulus should be carefully carried out [126]. In this direction the biodegradation and fate of the delivery vehicles and their encapsulated cargo are important factors to consider [127]. It is essential to ensure that the physicochemical properties of the carrier remain integral before its delivery to the target site. Ideally, upon external stimulus the drug to be delivered would be released and the matrix of the carrier vehicle would be degraded in a manner that it can be easily eliminate through the metabolism in a safe manner, deprived of immunological and toxic response [128,129].

Overall, stimuli-controlled release materials present potential benefits over conventional drug delivery approaches given by their great potential for improved delivery and treatment in a control and timely manner [130]. However, it still remains a challenge to describe which of the many approaches described in this review might be the next generation of stimulus response material to be able to translate to clinics.

Acknowledgments

N. F. acknowledges funding from the Swedish Innovation Agency (Vinnova). S. R. thanks Fazit Stiftung for a PhD fellowship. Z. L. is grateful to Chinese Scholarship Council (CSC) for a PhD fellowship. W. J. P. acknowledges the Deutsche Forschungsgemeinschaft for funding (DFG grant PA 794/21-1).

References

[1] J.M. Meacham, K. Durvasula, F.L. Degertekin, A.G. Fedorov, Physical methods for intracellular delivery: practical aspects from laboratory use to industrial-scale processing, J. Lab. Autom. 19 (2014) 1–18.
[2] Q. Sun, Z. Zhou, N. Qiu, Y. Shen, Rational design of cancer nanomedicine: nanoproperty integration and synchronization, Adv. Mater. 29 (2017), 1606628. .
[3] J. Siepmann, Fundamentals and applications of controlled release drug delivery, Springer US, Boston, MA, USA, 2012.
[4] B. Chang, D. Chen, Y. Wang, Y. Chen, Y. Jiao, X. Sha, W. Yang, Bioresponsive controlled drug release based on mesoporous silica nanoparticles coated with reductively sheddable polymer shell, Chem. Mater. 25 (2013) 574–585.
[5] Y. Ma, W.F. Dong, M.A. Hempenius, H. Möhwald, G.J. Vancso, Redox-controlled molecular permeability of composite-wall microcapsules, Nature Mater. 5 (2006) 724–729.
[6] W. Liao, C. Lu, R. Hartmann, F. Wang, Y.S. Sohn, W.J. Parak, I. Willner, Adenosine triphosphate-triggered release of macromolecular and nanoparticle loads from aptamer/DNA-cross-linked microcapsules, ACS Nano 9 (2015) 9078–9086.
[7] A. Ott, X. Yu, R. Hartmann, J. Rejman, A. Schütz, M. Ochs, W.J. Parak, S. Carregal Romero, Light-addressable and degradable silica capsules for delivery of molecular cargo to the cytosol of cells, Chem. Mater. 27 (2015) 1929–1942.
[8] Y. Wang, G. Wei, X. Zhang, F. Xu, X. Xiong, S. Zhou, A step-by-step multiple stimuli-responsive nanoplatform for enhancing combined chemo-photodynamic therapy, Adv. Mater. 29 (2017), 1605357. .
[9] Y.I. Golovin, S.L. Gribanovsky, D.Y. Golovin, N.L. Klyachko, A.G. Majouga, C. Master, M.S. A, A.V. Kabanov, Towards nanomedicines of the future: remote magneto-mechanical actuation of nanomedicines by alternating magnetic fields, J. Control. Release, 219 (2015) 43–60.
[10] L.L. del Mercato, E. Gonzalez, A.Z. Abbasi, W.J. Parak, V. Puntes, Synthesis and evaluation of gold nanoparticle-modified polyelectrolyte capsules under microwave irradiation for remotely controlled release for cargo, J. Mater. Chem. 21 (2011) 11468–11471.
[11] Y. Negishi, Y. Endo-Takahashi, Y. Matsuki, Y. Kato, N. Takagi, R. Suzuki, K. Maruyama, Y. Aramaki, Systemic delivery systems of angiogenic gene by novel bubble liposomes containing cationic lipid and ultrasound exposure, Mol. Pharm. 9 (2012) 1834–1840.
[12] K. Un, S. Kawakami, R. Suzuki, K. Maruyama, F. Yamashita, M. Hashida, Suppression of melanoma growth and metastasis by DNA vaccination using an ultrasound-responsive and mannose-modified gene carrier, Mol. Pharm. 8 (2011) 543–554.
[13] Q. Yan, J. Yuan, Z. Cai, Y. Xin, Y. Kang, Y. Yin, Voltage-responsive vesicles based on orthogonal assembly of two homopolymers, J. Am. Chem. Soc. 132 (2010) 9268–9270.
[14] H. Kim, S.M. Jeong, J.W. Park, Electrical switching between vesicles and micelles via redox-responsive self-assembly of amphiphilic rod−coils, J. Am. Chem. Soc. 133 (2011) 5206–5209.
[15] J. Ge, E. Neofytou, T.J. Cahill III, R.E. Beygui, R.N. Zare, Drug release from electric-field-responsive nanoparticles, ACS Nano 6 (2011) 227–233.
[16] A.G. Skirtach, C. Dejugnat, D. Braun, A.S. Susha, W.J. Parak, H. Möhwald, G.B. Sukhorukov, The role of metal nanoparticles in remote release of encapsulated materials, Nano Lett. 5 (2005) 1371–1377.
[17] S. Carregal-Romero, P. Guardia, X. Yu, R. Hartmann, T. Pellegrino, W.J. Parak, Magnetically triggered release of molecular cargo from iron oxide nanoparticle loaded microcapsules, Nanoscale 7 (2015) 570–576.
[18] M. Nair, R. Guduru, P. Liang, J. Hong, V. Sagar, S. Khizroev, Externally controlled on-demand release of anti-HIV drug using magneto-electric nanoparticles as carriers, Nat. Commun. 4 (2013) 1707.
[19] A. Barhoumi, Q. Liu, D.S. Kohane, Ultraviolet light-mediated drug delivery: principles, applications, and challenges, J. Control. Release 219 (2015) 31–42.
[20] L. Li, X. Deng, Z. Li, F. Du, Z. Li, Multifunctional photodegradable polymers for reactive micropatterns, Macromolecules 47 (2014) 4660–4667.
[21] A. Bagheri, J. Yeow, H. Arandiyan, J. Xu, C. Boyer, M. Lim, Polymerization of a photocleavable monomer using visible light, Macromol. Rapid Commun. 37 (2016) 905–910.
[22] A.n. Jiménez-Balsa, S. Pinto, E. Quartin, M.M. Lino, V. Francisco, L. Ferreira, Nanoparticles conjugated with photocleavable linkers for the intracellular delivery of biomolecules, Bioconjug. Chem. 29 (2018) 1485–1489.
[23] P. Juzenas, A. Juzeniene, O. Kaalhus, V. Iani, J. Moan, Noninvasive fluorescence excitation spectroscopy during application of 5-aminolevulinic acid in vivo, Photochem. Photobiol. Sci. 1 (2002) 745–748.
[24] D.L. Mitchell, J. Jen, J.E. Cleaver, Relative induction of cyclobutane dimers and cytosine photohydrates in DNA irradiated in vitro and in vivo with ultraviolet-C and ultraviolet-B light, Photochem. Photobiol. 54 (1991) 741–746.
[25] M. Qiu, D. Wang, W. Liang, L. Liu, Y. Zhang, X. Chen, D.K. Sang, C. Xing, Z. Li, B. Dong, Novel concept of the smart NIR-light–controlled drug release of black phosphorus nanostructure for cancer therapy, Proc. Natl. Acad. Sci. 115 (2018) 501–506.
[26] T.S. Stewart, A. Nagesetti, R. Guduru, P. Liang, E. Stimphil, A. Hadjikhani, L. Salgueiro, J. Horstmyer, R. Cai, A. Schally, Magnetoelectric nanoparticles for delivery of antitumor peptides into glioblastoma cells by magnetic fields, Nanomedicine 13 (2018) 423–438.
[27] R. Guduru, P. Liang, C. Runowicz, M. Nair, V. Atluri, S. Khizroev, Magneto-electric nanoparticles to enable field-controlled high-specificity drug delivery to eradicate ovarian cancer cells, Sci. Rep. 3 (2013) 2953.
[28] A. Rodzinski, R. Guduru, P. Liang, A. Hadjikhani, T. Stewart, E. Stimphil, C. Runowicz, R. Cote, N. Altman, R. Datar, Targeted and controlled anticancer drug delivery and release with magnetoelectric nanoparticles, Sci. Rep. 6 (2016), 20867. .
[29] Z. Zhou, X. Liu, D. Zhu, Y. Wang, Z. Zhang, X. Zhou, N. Qiu, X. Chen, Y. Shen, Nonviral cancer gene therapy: delivery cascade and vector nanoproperty integration, Adv. Drug Del. Rev. 115 (2017) 115–154.
[30] R. Hartmann, M. Weidenbach, M. Neubauer, A. Fery, W.J. Parak, Stiffness-dependent in vitro uptake and lysosomal acidification of colloidal particles, Angew. Chem. Int. Ed. 54 (2015) 1365–1368.
[31] L. Kastl, D. Sasse, V. Wulf, R. Hartmann, J. Mircheski, C. Ranke, S. Carregal-Romero, J.A. Martínez-López, R. Fernández-Chacón, W.J. Parak, H.-P. Elsaesser, P. Rivera Gil, Multiple internalization pathways of polyelectrolyte multilayer capsules into mammalian cells, ACS Nano 7 (2013) 6605–6618.
[32] J. Gilleron, W. Querbes, A. Zeigerer, A. Borodovsky, G. Marsico, U. Schubert, K. Manygoats, S. Seifert, C. Andree, M. Stöter, Image-based analysis of lipid nanoparticle–mediated siRNA delivery, intracellular trafficking and endosomal escape, Nat. Biotechnol. 31 (2013) 638–646.
[33] D. Zhu, H. Yan, X. Liu, J. Xiang, Z. Zhou, J. Tang, X. Liu, Y. Shen, Intracellularly disintegratable polysulfoniums for efficient gene delivery, Adv. Funct. Mater. 27 (2017), 1606826. .
[34] H. Yan, D. Zhu, Z. Zhou, X. Liu, Y. Piao, Z. Zhang, X. Liu, J. Tang, Y. Shen, Facile synthesis of semi-library of low charge density cationic polyesters from poly (alkylene maleate)s for efficient local gene delivery, Biomaterials 178 (2018) 559–569.
[35] Q. Jiang, D. Yue, Y. Nie, X. Xu, Y. He, S. Zhang, E. Wagner, Z. Gu, Specially-made lipid-based assemblies for improving transmembrane gene delivery: comparison of basic amino acid residue rich periphery, Mol. Pharm. 13 (2016) 1809–1821.
[36] A. Quarta, M. Rodio, M. Cassani, G. Gigli, T. Pellegrino, L.L. del Mercato, Multilayered magnetic nanobeads for the delivery of peptides molecules triggered by intracellular proteases, ACS Appl. Mater. Inter. 9 (2017) 35095–35104.
[37] P.R. Gil, S.D. Koker, B.G.D. Geest, W.J. Parak, Intracellular processing of proteins mediated by biodegradable polyelectrolyte capsules, Nano Lett. 9 (2009) 4398–4402.
[38] S. Carregal-Romero, M. Ochs, P. Rivera Gil, C. Ganas, A.M. Pavlov, G.B. Sukhorukov, W.J. Parak, NIR-light triggered delivery of macromolecules into the cytosol, J. Control. Release 159 (2012) 120–127.
[39] Z.u. Rehman, D. Hoekstra, I.S. Zuhorn, Mechanism of polyplex-and lipoplex-mediated delivery of nucleic acids: real-time visualization of transient membrane destabilization without endosomal lysis, ACS Nano 7 (2013) 3767–3777.
[40] K. Han, Q. Lei, H.Z. Jia, S.B. Wang, W.N. Yin, W.H. Chen, S.X. Cheng, X.Z. Zhang, A tumor targeted chimeric peptide for synergistic endosomal escape and therapy by dual-stage light manipulation, Adv. Funct. Mater. 25 (2015) 1248–1257.
[41] M. Ochs, S. Carregal Romero, J. Rejman, K. Braeckmans, S.C. De Smedt, W.J. Parak, Light-addressable capsules as caged compound matrix for controlled in vitro release, Angew. Chem. Int. Ed. 52 (2013) 695–699.

[42] P.T. Wong, S. Tang, J. Cannon, D. Chen, R. Sun, J. Lee, J. Phan, K. Tao, K. Sun, B. Chen, Photocontrolled release of doxorubicin conjugated through a thioacetal photocage in folate-targeted nanodelivery systems, Bioconjug. Chem. 28 (2017) 3016–3028.
[43] W. Ji, N. Li, D. Chen, X. Qi, W. Sha, Y. Jiao, Q. Xu, J. Lu, Coumarin-containing photo-responsive nanocomposites for NIR light-triggered controlled drug release via a two-photon process, J. Mater. Chem. B 1 (2013) 5942–5949.
[44] C.J. Carling, M.L. Viger, V.A.N. Huu, A.V. Garcia, A. Almutairi, In vivo visible light-triggered drug release from an implanted depot, Chem.Sci. 6 (2015) 335–341.
[45] C. Englert, I. Nischang, C. Bader, P. Borchers, J. Alex, M. Prçhl, M. Hentschel, M. Hartlieb, A. Traeger, G. Pohnert, Photocontrolled release of chemicals from nano- and microparticle containers, Angew. Chem. Int. Ed. 57 (2018) 2479–2482.
[46] B.R. Sarode, K. Kover, P.Y. Tong, C. Zhang, S.H. Friedman, Light control of insulin release and blood glucose using an injectable photoactivated depot, Mol. Pharm. 13 (2016) 3835–3841.
[47] R. Tong, H.H. Chiang, D.S. Kohane, Photoswitchable nanoparticles for in vivo cancer chemotherapy, Proc. Natl. Acad. Sci. 110 (2013) 19048–19053.
[48] Y.T. Chang, P.Y. Liao, H.S. Sheu, Y.J. Tseng, F.Y. Cheng, C.S. Yeh, Near-infrared light-responsive intracellular drug and siRNA release using au nanoensembles with oligonucleotide-capped silica shell, Adv. Mater. 24 (2012) 3309–3314.
[49] Z. Xiao, C. Ji, J. Shi, E.M. Pridgen, J. Frieder, J. Wu, O.C. Farokhzad, DNA self-assembly of targeted near-infrared-responsive gold nanoparticles for cancer thermo-chemotherapy, Angew. Chem. Int. Ed. 124 (2012) 12023–12027.
[50] H. Kim, H. Lee, K.Y. Seong, E. Lee, S.Y. Yang, J. Yoon, Visible light-triggered on-demand drug release from hybrid hydrogels and its application in transdermal patches, Adv. Healthc. Mater. 4 (2015) 2071–2077.
[51] Y. Yuan, C.J. Zhang, B. Liu, A photoactivatable AIE polymer for light-controlled gene delivery: concurrent endo/lysosomal escape and DNA unpacking, Angew. Chem. Int. Ed. 54 (2015) 11419–11423.
[52] S. Mura, J. Nicolas, P. Couvreur, Stimuli-responsive nanocarriers for drug delivery, Nature Mater. 12 (2013) 991–1003.
[53] Y. Becker, E. Unger, M.A. Fichte, D.A. Gacek, A. Dreuw, J. Wachtveitl, P.J. Walla, A. Heckel, A red-shifted two-photon-only caging group for three-dimensional photorelease, Chem.Sci. 9 (2018) 2797–2802.
[54] B. Yan, J.-C. Boyer, N.R. Branda, Y. Zhao, Near-infrared light-triggered dissociation of block copolymer micelles using upconverting nanoparticles, J. Am. Chem. Soc. 133 (2011) 19714–19717.
[55] J. Olejniczak, C.-J. Carling, A. Almutairi, Photocontrolled release using one-photon absorption of visible or NIR light, J. Control. Release 219 (2015) 18–30.
[56] H. Chen, L. Xiao, Y. Anraku, P. Mi, X. Liu, H. Cabral, A. Inoue, T. Nomoto, A. Kishimura, N. Nishiyama, Polyion complex vesicles for photoinduced intracellular delivery of amphiphilic photosensitizer, J. Am. Chem. Soc. 136 (2013) 157–163.
[57] T. Nomoto, S. Fukushima, M. Kumagai, K. Machitani, Y. Matsumoto, M. Oba, K. Miyata, K. Osada, N. Nishiyama, K. Kataoka, Three-layered polyplex micelle as a multifunctional nanocarrier platform for light-induced systemic gene transfer, Nat. Commun. 5 (2014) 3545.
[58] N. Nishiyama, A. Iriyama, W. Jang, K. Miyata, K. Itaka, Y. Inoue, H. Takahashi, Y. Yanagi, Y. Tamaki, H. Koyama, Light-induced gene transfer from packaged DNA enveloped in a dendrimeric photosensitizer, Nature Mater. 4 (2005) 934–941.
[59] A.Y. Rwei, J.J. Lee, C. Zhan, Q. Liu, M.T. Ok, S.A. Shankarappa, R. Langer, D.S. Kohane, Repeatable and adjustable on-demand sciatic nerve block with phototriggerable liposomes, Proc. Natl. Acad. Sci. 112 (2015) 15719–15724.
[60] K.A. Carter, S. Shao, M.I. Hoopes, D. Luo, B. Ahsan, V.M. Grigoryants, W. Song, H. Huang, G. Zhang, R.K. Pandey, Porphyrin–phospholipid liposomes permeabilized by near-infrared light, Nat. Commun. 5 (2014) 3546.
[61] A.E. Vasdekis, E.A. Scott, C.P. O'Neil, D. Psaltis, J.A. Hubbell, Precision intracellular delivery based on optofluidic polymersome rupture, ACS Nano 6 (2012) 7850–7857.
[62] A.G. Skirtach, A.M. Javier, O. Kreft, K. Köhler, A.P. Alberola, H. Möhwald, W.J. Parak, G.B. Sukhorukov, Laser-induced release of encapsulated materials inside living cells, Angew. Chem. Int. Ed. 45 (2006) 4612–4617.
[63] A.G. Skirtach, A.A. Antipov, D.G. Shchukin, G.B. Sukhorukov, Remote activation of capsules containing Ag nanoparticles and IR dye by laser light, Langmuir 20 (2004) 6988–6992.
[64] A. Muñoz Javier, P. del Pino, M.F. Bedard, A.G. Skirtach, D. Ho, G.B. Sukhorukov, C. Plank, W.J. Parak, Photoactivated release of cargo from the cavity of polyelectrolyte capsules to the cytosol of cells, Langmuir 24 (2008) 12517–12520.
[65] B. Radt, T.A. Smith, F. Caruso, Optically addressable nanostructured capsules, Adv. Mater. 16 (2004) 2184–2189.
[66] R. Palankar, A.G. Skirtach, O. Kreft, M. Bedard, M. Garstka, K. Gould, H. Mohwald, G.B. Sukhorukov, M. Winterhalter, S. Springer, Controlled intracellular release of peptides from microcapsules enhances antigen presentation on MHC class I molecules, Small 5 (2009) 2168–2176.
[67] D. Hühn, A. Govorov, P. Rivera Gil, W.J. Parak, Photostimulated au nanoheaters in polymer and biological media: characterization of mechanical destruction and boiling, Adv. Funct. Mater. 22 (2012) 294–303.
[68] J. Huang, K.S. Jackson, C.J. Murphy, Polyelectrolyte wrapping layers control rates of photothermal molecular release from gold nanorods, Nano Lett. 12 (2012) 2982–2987.
[69] L.L. del Mercato, P. Rivera Gil, A.Z. Abbasi, M. Ochs, C. Ganas, I. Zins, C. Sönnichsen, W.J. Parak, LbL multilayer capsules: recent progress and future outlook for their use in life sciences, Nanoscale 2 (2010) 458–467.
[70] K. Kantner, J. Rejman, K.V.L. Kraf, M.G. Soliman, M.V. Zyuzin, A. Escudero, P.d. Pino, W.J. Parak, Laterally and temporally controlled intracellular staining by light-triggered release of encapsulated fluorescent markers, Chem. Eur. J. 24 (2018) 2098–2102.
[71] A. Ambrosone, V. Marchesano, S. Carregal-Romero, D. Intartaglia, W.J. Parak, C. Tortiglione, Control of wnt/β-catenin signaling pathway in vivo via light responsive capsules, ACS Nano 10 (2016) 4828–4834.
[72] G. Kaufman, K.A. Montejo, A. Michaut, P.W. Majewski, C.O. Osuji, Photoresponsive and magnetoresponsive graphene oxide microcapsules fabricated by droplet microfluidics, ACS Appl. Mater. Inter. 9 (2017) 44192–44198.
[73] R. Kurapati, A.M. Raichur, Near-infrared light-responsive graphene oxide composite multilayer capsules: a novel route for remote controlled drug delivery, Chem. Commun. 49 (2013) 734–736.
[74] M. Hashemi, M. Omidi, B. Muralidharan, L. Tayebi, M.J. Herpin, M.A. Mohagheghi, J. Mohammadi, H.D. Smyth, T.E. Milner, Layer-by-layer assembly of graphene oxide on thermosensitive liposomes for photo-chemotherapy, Acta Biomater. 65 (2018) 376–392.
[75] L.L. del Mercato, F. Guerra, G. Lazzari, C. Nobile, C. Bucci, R. Rinaldi, Biocompatible multilayer capsules engineered with a graphene oxide derivative: synthesis, characterization and cellular uptake, Nanoscale 8 (2016) 7501–7512.
[76] K.A. Dendramis, D.T. Chiu, Laser photolysis of dye-sensitized nanocapsules occurs via a photothermal pathway, J. Am. Chem. Soc. 131 (2009) 16771–16778.
[77] S. Su, Y. Tian, Y. Li, Y. Ding, T. Ji, M. Wu, Y. Wu, G. Nie, "Triple-punch" strategy for triple negative breast cancer therapy with minimized drug dosage and improved antitumor efficacy, ACS Nano 9 (2015) 1367–1378.
[78] G.V. Orsinger, J.D. Williams, M. Romanowski, Focal activation of cells by plasmon resonance assisted optical injection of signaling molecules, ACS Nano 8 (2014) 6151–6162.
[79] T.S. Troutman, J.K. Barton, M. Romanowski, Biodegradable plasmon resonant nanoshells, Adv. Mater. 20 (2008) 2604–2608.
[80] X. Li, Z. Che, K. Mazhar, T.J. Price, Z. Qin, Ultrafast near-infrared light-triggered intracellular uncaging to probe cell signaling, Adv. Funct. Mater. 27 (2017), 1605778. .
[81] G. Wu, A. Mikhailovsky, H.A. Khant, C. Fu, W. Chiu, J.A. Zasadzinski, Remotely triggered liposome release by near-infrared light absorption via hollow gold nanoshells, J. Am. Chem. Soc. 130 (2008) 8175–8177.
[82] A.M. Goodman, O. Neumann, K. Nørregaard, L. Henderson, M.-R. Choi, S.E. Clare, N.J. Halas, Near-infrared remotely triggered drug-release strategies for cancer treatment, Proc. Natl. Acad. Sci. 114 (2017) 12419–12424.
[83] A. Barhoumi, R. Huschka, R. Bardhan, M.W. Knight, N.J. Halas, Light-induced release of DNA from plasmon-resonant nanoparticles: towards light-controlled gene therapy, Chem. Phys. Lett. 482 (2009) 171–179.
[84] R. Huschka, J. Zuloaga, M.W. Knight, L.V. Brown, P. Nordlander, N.J. Halas, Light-induced release of DNA from gold nanoparticles: nanoshells and nanorods, J. Am. Chem. Soc. 133 (2011) 12247–12255.
[85] A.S. Urban, T. Pfeiffer, M. Fedoruk, A.A. Lutich, J. Feldmann, Single-step injection of gold nanoparticles through phospholipid membranes, ACS Nano 5 (2011) 3585–3590.
[86] S.J. Leung, M. Romanowski, Molecular catch and release: controlled delivery using optical trapping with light-responsive liposomes, Adv. Mater. 24 (2012) 6380–6383.
[87] S. Johannsmeier, P. Heeger, M. Terakawa, S. Kalies, A. Heisterkamp, T. Ripken, D. Heinemann, Gold nanoparticle-mediated laser stimulation induces a complex stress response in neuronal cells, Sci. Rep. 8 (2018) 6533.
[88] L. Gentemann, S. Kalies, M. Coffee, H. Meyer, T. Ripken, A. Heisterkamp, R. Zweigerdt, D. Heinemann, Modulation of cardiomyocyte activity using pulsed laser irradiated gold nanoparticles, Biomed. Opt. Express 8 (2017) 177–192.
[89] M. Garstka, B. Borchert, M. Al-Balushi, P. Praveen, N. Kühl, I. Majoul, R. Duden, S. Springer, Peptide-receptive major histocompatibility complex class I molecules cycle between endoplasmic reticulum and cis-Golgi in wild-type lymphocytes, J. Biol. Chem. 282 (2007) 30680–30690.
[90] A. Townsend, H. Bodmer, Antigen recognition by class I-restricted T lymphocytes, Annu. Rev. Immunol. 7 (1989) 601–624.
[91] S.J. Leung, M. Romanowski, NIR-activated content release from plasmon resonant liposomes for probing single-cell responses, ACS Nano 6 (2012) 9383–9391.
[92] K.A. Gregersen, Z.B. Hill, J.C. Gadd, B.S. Fujimoto, D.J. Maly, D.T. Chiu, Intracellular delivery of bioactive molecules using light-addressable nanocapsules, ACS Nano 4 (2010) 7603–7611.
[93] Y. Zhang, L. Huang, Z. Li, G. Ma, Y. Zhou, G. Han, Illuminating cell signaling with near-infrared light-responsive nanomaterials, ACS Nano 10 (2016) 3881–3885.
[94] G.B. Braun, A. Pallaoro, G.H. Wu, D. Missirlis, J.A. Zasadzinski, M. Tirrell, N.O. Reich, Laser-activated gene silencing via gold nanoshell-siRNA conjugates, ACS Nano 3 (2009) 2007–2015.
[95] J.X. Shao, M.J. Xuan, T.Y. Si, L.R. Dai, Q. He, Biointerfacing polymeric microcapsules for in vivo near-infrared light-triggered drug release, Nanoscale 7 (2015) 19092–19098.
[96] R. Di Corato, A. Espinosa, L. Lartigue, M. Tharaud, S. Chat, T. Pellegrino, C. Menager, F. Gazeau, C. Wilhelm, Magnetic hyperthermia efficiency in the cellular environment for different nanoparticle designs, Biomaterials 35 (2014) 6400–6411.
[97] P. Guardia, R. Di Corato, L. Lartigue, C. Wilhelm, A. Espinosa, M. Garcia-Hernandez, F. Gazeau, L. Manna, T. Pellegrino, Water-soluble iron oxide nanocubes with high values of specific absorption rate for cancer cell hyperthermia treatment, ACS Nano 6 (2012) 3080–3091.
[98] N. Hallali, P. Clerc, D. Fourmy, V. Gigoux, J. Carrey, Influence on cell death of high frequency motion of magnetic nanoparticles during magnetic hyperthermia experiments, Appl. Phys. Lett. 109 (2016), 032402. .
[99] V. Connord, P. Clerc, N. Hallali, D. El Hajj Diab, D. Fourmy, V. Gigoux, J. Carrey, Real-time analysis of magnetic hyperthermia rxperiments on living vells under a vonfocal microscope, Small 11 (2015) 2437–2445.

[100] R.E. Rosensweig, Heating magnetic fluid with alternating magnetic field, J. Magn. Magn. Mater. 252 (2002) 370–374.
[101] K. Katagiri, M. Nakamura, K. Koumoto, Magnetoresponsive smart capsules formed with polyelectrolytes, lipid bilayers and magnetic nanoparticles, ACS Appl. Mater. Inter. 2 (2010) 768–773.
[102] S.H. Hu, C.H. Tsai, C.F. Liao, D.M. Liu, S.Y. Chen, Controlled rupture of magnetic polyelectrolyte microcapsules for drug delivery, Langmuir 24 (2008) 11811–11818.
[103] Z. Lu, M.D. Prouty, Z. Guo, V.O. Golub, C.S. Kumar, Y.M. Lvov, Magnetic switch of permeability for polyelectrolyte microcapsules embedded with Co@au nanoparticles, Langmuir 21 (2005) 2042–2050.
[104] K. Katagiri, Y. Imai, K. Koumoto, T. Kaiden, K. Kono, S. Aoshima, Magnetoresponsive on-demand release of hybrid liposomes formed from Fe_3O_4 nanoparticles and hyhermosensitive block copolymers, Small 7 (2011) 1683–1689.
[105] H. Oliveira, E. Pérez-Andrés, J. Thevenot, O. Sandre, E. Berra, S. Lecommandoux, Magnetic field triggered drug release from polymersomes for cancer therapeutics, J. Control. Release 169 (2013) 165–170.
[106] T.T.T. N'Guyen, H.T.T. Duong, J. Basuki, V. Montembault, S. Pascual, C. Guibert, J. Fresnais, C. Boyer, M.R. Whittaker, T.P. Davis, L. Fontaine, Functional iron oxide magnetic nanoparticles with hyperthermia-induced drug release ability by using a combination of orthogonal click reactions, Angew. Chem. Int. Ed. 52 (2013) 14152–14156.
[107] A. Riedinger, P. Guardia, A. Curcio, M.A. Garcia, R. Cingolani, L. Manna, T. Pellegrino, Subnanometer local temperature probing and remotely controlled drug release based on azo-functionalized iron oxide nanoparticles, Nano Lett. 13 (2013) 2399–2406.
[108] K. Ang, S. Venkatraman, R. Ramanujan, Magnetic PNIPA hydrogels for hyperthermia applications in cancer therapy, Mater. Sci. Eng. C 27 (2007) 347–351.
[109] K. Hayashi, K. Ono, H. Suzuki, M. Sawada, M. Moriya, W. Sakamoto, T. Yogo, High-frequency, magnetic-field-responsive drug release from magnetic nanoparticle/organic hybrid based on hyperthermic effect, ACS Appl. Mater. Inter. 2 (2010) 1903–1911.
[110] S.H. Hu, Y.Y. Chen, T.C. Liu, T.H. Tung, D.M. Liu, S.Y. Chen, Remotely nanorupturable yolk/shell capsules for magnetically-triggered drug release, Chem. Commun. 47 (2011) 1776–1778.
[111] S.H. Hu, D.M. Liu, W.L. Tung, C.F. Liao, S.Y. Chen, Surfactant-free, self-assembled PVA-iron oxide/silica core–shell nanocarriers for highly sensitive, magnetically controlled drug release and ultrahigh cancer cell uptake efficiency, Adv. Funct. Mater. 18 (2008) 2946–2955.
[112] L.H. Reddy, J.L. Arias, J. Nicolas, P. Couvreur, Magnetic nanoparticles: design and characterization, toxicity and biocompatibility, pharmaceutical and biomedical applications, Chem. Rev. 112 (2012) 5818–5878.
[113] J.T. Dias, M. Moros, P. del Pino, S. Rivera, V. Grazú, J.M. de la Fuente, DNA as a molecular local thermal probe for the analysis of magnetic hyperthermia, Angew. Chem. Int. Ed. 52 (2013) 11526–11529.
[114] A.M. Derfus, G. von Maltzahn, T.J. Harris, T. Duza, K.S. Vecchio, E. Ruoslahti, S.N. Bhatia, Remotely triggered release from magnetic nanoparticles, Adv. Mater. 19 (2007) 3932–3936.
[115] E. Ruiz-Hernandez, A. Baeza, M. Vallet-Regi, Smart drug delivery through DNA/magnetic nanoparticle gates, ACS Nano 5 (2011) 1259–1266.
[116] C.R. Thomas, D.P. Ferris, J.H. Lee, E. Choi, M.H. Cho, E.S. Kim, J.F. Stoddart, J.S. Shin, J. Cheon, J.I. Zink, Noninvasive remote-controlled release of drug molecules in vitro using magnetic actuation of mechanized nanoparticles, J. Am. Chem. Soc. 132 (2010) 10623–10625.
[117] P. Saint-Cricq, S. Deshayes, J. Zink, A. Kasko, Magnetic field activated drug delivery using thermodegradable azo-functionalised PEG-coated core–shell mesoporous silica nanoparticles, Nanoscale 7 (2015) 13168–13172.
[118] E. Bringas, O. Koysuren, D.V. Quach, M. Mahmoudi, E. Aznar, J.D. Roehling, M.D. Marcos, R. Martinez-Manez, P. Stroeve, Triggered release in lipid bilayer-capped mesoporous silica nanoparticles containing SPION using an alternating magnetic field, Chem. Commun. 48 (2012) 5647–5649.
[119] S. Hu, S. Chen, X. Gao, Multifunctional nanocapsules for simultaneous encapsulation of hydrophilic and hydrophobic compounds and on-demand release, ACS Nano 6 (2012) 2558–2565.
[120] J. Young, M. Wang, I. Brezovich, Frequency/depth-penetration considerations in hyperthermia by magnetically induced currents, Electron. Lett. 16 (1980) 358–359.
[121] E.C. Abenojar, S. Wickramasinghe, M. Ju, S. Uppaluri, A. Klika, J. George, W. Barsoum, S.J. Frangiamore, C.A. Higuera-Rueda, A.C.S. Samia, Magnetic glycol chitin-based hydrogel nanocomposite for combined thermal and d-amino-acid-assisted biofilm disruption, ACS Infect. Dis. 4 (2018) 1246–1256.
[122] J.C. Castillo-Martínez, G.A. Martínez-Castañón, F. Martínez-Gutierrez, N.V. Zavala-Alonso, N. Patiño-Marín, N. Niño-Martinez, V. Zaragoza-Magaña, C. Cabral-Romero, Antibacterial and antibiofilm activities of the photothermal therapy using gold nanorods against seven different bacterial strains, J. Nanomater. 2015 (2015), 783671. .
[123] J. Morales-Dalmau, C. Vilches, I.d. Miguel, V. Sanza, R. Quidant, Optimum morphology of gold nanorods for lightinduced hyperthermia, Nanoscale, 10 (2018) 2632–2638.
[124] Q. Zhang, I. Castellanos-Rubio, R. Munshi, I. Orue, B. Pelaz, K.I. Gries, W.J. Parak, P.d. Pino, A. Pralle, Model driven optimization of magnetic anisotropy of exchange-coupled core-shell ferrite nanoparticles for maximal hysteretic loss, Chem. Mater. 27 (2015) 7380–7387.
[125] H. Gu, S. Mu, G. Qiu, X. Liu, L. Zhang, Y. Yuan, D. Astruc, Redox-stimuli-responsive drug delivery systems with supramolecular ferrocenyl-containing polymers for controlled release, Coord. Chem. Rev. 364 (2018) 51–85.
[126] N. Feliu, J. Hühn, M.V. Zyuzin, S. Ashraf, D. Valdeperez, A. Masood, A.H. Said, A. Escudero, B. Pelaz, E. Gonzalez, M.A.C. Duarte, S. Roy, I. Chakraborty, M.L. Lim, S. Sjöqvist, P. Jungebluth, W.J. Parak, Quantitative uptake of colloidal particles by cell cultures, Sci. Total Environ. 568 (2016) 819–828.
[127] N. Feliu, D. Docter, M. Heine, P. del Pino, S. Ashraf, J. Kolosnjaj-Tabi, P. Macchiarini, P. Nielsen, D. Alloyeau, F. Gazeau, In vivo degeneration and the fate of inorganic nanoparticles, Chem. Soc. Rev. 45 (2016) 2440–2457.
[128] N. Feliu, M.V. Walter, M.I. Montanez, A. Kunzmann, A. Hult, A. Nystrom, M. Malkoch, B. Fadeel, Stability and biocompatibility of a library of polyester dendrimers in comparison to polyamidoamine dendrimers, Biomaterials 33 (2012) 1970–1981.
[129] C. Ding, L. Tong, J. Feng, J. Fu, Recent advances in stimuli-responsive release function drug delivery systems for tumor, Molecules 21 (2016) 1715.
[130] M.J. Ernsting, M. Murakami, A. Roy, S.D. Li, Factors controlling the pharmacokinetics, biodistribution and intratumoral penetration of nanoparticles, J. Control. Release 172 (2013) 782–794.